Growth and development in Toxoplasma gondii
by Michael Nicholas Guerini

A dissertation submitted in partial fulfillment of the requirements for the degree of Doctor of Philosophy in Veterinary Molecular Biology
Montana State University

Abstract:
The significance of Toxoplasma gondii to human and animal health, along with its value as a model for other pathogenic protozoa, makes this microorganism an important model in the field of Apicomplexa research. It is clear from numerous studies of the diseases caused by this family of microorganisms that parasitaemia itself is key to pathogenesis, and thus, an understanding of the growth processes in these pathogens could provide better treatments. In this work, the relationship/regulation between the cell cycle and development was investigated. A G2 population arose during tachyzoite-to-bradyzoite differentiation thus, providing a mechanism of linking the cell cycle with development. To gain further insight into the regulation of the parasite cell cycle, both a reverse and forward genetic approach was used. One approach used bioinformatics and cDNA library screening to identify cell cycle related proteins. Two distinct proliferating cell nuclear antigen (PCNA) genes in T. gondii were identified and this work demonstrated that these two genes were differentially expressed during development and the tachyzoite cell cycle. Further work showed that each PCNA likely acts independently and provided evidence that TgPCNA1 potentially serves as the major replisomal PCNA. The function of PCNA2 in T. gondii remains unknown. Finally, a forward genetics approach focused on the complementation of the tachyzoite temperature sensitive (ts) mutant 11C9, which arrests within 1 to 2 divisions at the non-permissive temperature (40°C), and approximately half of the parasites arrest with a single undivided nucleus (2N) placing the defect at some point in mitosis. Complementation of tel 11C9 with a homolog of the eukaryotic XPMC2 suggests that the cyclinB/cdk or wee1/chk1 pathway in this mutant is likely affected. In T. gondii, a proposed linkage between growth and development seem consistent with a developmental timer system (“clock mechanism”), yet the presence of checkpoints suggests that the domino model plays at least a partial role in regulating the tachyzoite cell cycle.

GROWTH AND DEVELOPMENT

IN *TOXOPLASMA GONDII*

by

Michael Nicholas Guerini

A dissertation submitted in partial fulfillment
of the requirements for the degree

of

Doctor of Philosophy

in

Veterinary Molecular Biology

MONTANA STATE UNIVERSITY
Bozeman, Montana

April 2002

APPROVAL

of a dissertation submitted by

Michael Nicholas Guerini

This dissertation has been read by each member of the dissertation committee and has been found to be satisfactory regarding content, English usage, format, citations, bibliographic style, and consistency, and is ready for submission to the College of Graduate studies.

Michael W. White Michael W. White 4-09-02
(Signature) Date

Approved for the Department of Veterinary Molecular Biology

Allen Harmsen Allen S. Harmsen 4/09/02
(Signature) Date

Approved for the College of Graduate Studies

Bruce R. McLeod Bruce R. McLeod 4-9-02
(Signature) Date

STATEMENT OF PERMISSION TO USE

In presenting this dissertation in partial fulfillment of the requirements for a doctoral degree at Montana State University-Bozeman, I agree that the Library shall make it available to borrowers under rules of the Library.

I further agree that copying of this dissertation is allowable only for scholarly purposes, consistent with "fair use" as prescribed in the U.S. Copyright Law. Requests for extensive copying or reproduction of this thesis should be referred to Bell and Howell Information and Learning, 300 North Zeeb Road, Ann Arbor, Michigan 48106, to whom I have granted "the exclusive right to reproduce and distribute my dissertation in and from microform along with the non-exclusive right to reproduce and distribute my abstract in any format in whole or in part."

Signature Michael Nicholas Gurnis

Date 4/9/02

ACKNOWLEDGMENTS

The accomplishment of completing my Ph.D. resulted from the efforts of numerous people. The most important contributions have come through encouragement, support and friendship.

I thank Albert and Barbara Guerini for emotional and financial support. I also thank Carla and Rick Wiesend, and Randy and Tammy Crone for being true friends and giving me the support and encouragement during some of the difficult times. My final thanks go to Dr. Rob Keene and Bart Goodman who fed me and kept me entertained.

Finally, I appreciate the help I received on the technical aspects of my dissertation from all involved, especially:

Maria Jerome

Jay Radke

Chris Kvaal

Xuchu Que

Sharon Reed

TABLE OF CONTENTS

LIST OF TABLES

LIST OF FIGURES

ABSTRACT

The significance of *Toxoplasma gondii* to human and animal health, along with its value as a model for other pathogenic protozoa, makes this microorganism an important model in the field of Apicomplexa research. It is clear from numerous studies of the diseases caused by this family of microorganisms that parasitaemia itself is key to pathogenesis, and thus, an understanding of the growth processes in these pathogens could provide better treatments. In this work, the relationship/regulation between the cell cycle and development was investigated. A G2 population arose during tachyzoite-to-bradyzoite differentiation thus, providing a mechanism of linking the cell cycle with development. To gain further insight into the regulation of the parasite cell cycle, both a reverse and forward genetic approach was used. One approach used bioinformatics and cDNA library screening to identify cell cycle related proteins. Two distinct proliferating cell nuclear antigen (PCNA) genes in *T. gondii* were identified and this work demonstrated that these two genes were differentially expressed during development and the tachyzoite cell cycle. Further work showed that each PCNA likely acts independently and provided evidence that TgPCNA1 potentially serves as the major replisomal PCNA. The function of PCNA2 in *T. gondii* remains unknown. Finally, a forward genetics approach focused on the complementation of the tachyzoite temperature sensitive (*ts*) mutant 11C9, which arrests within 1 to 2 divisions at the non-permissive temperature (40°C), and approximately half of the parasites arrest with a single undivided nucleus (2N) placing the defect at some point in mitosis. Complementation of *ts*11C9 with a homolog of the eukaryotic XPMC2 suggests that the cyclinB/cdk or wee1/chk1 pathway in this mutant is likely affected. In *T. gondii*, a proposed linkage between growth and development seem consistent with a developmental timer system ("clock mechanism"), yet the presence of checkpoints suggests that the domino model plays at least a partial role in regulating the tachyzoite cell cycle.

CHAPTER 1

TOXOPLASMA GONDII AND APICOMPLEXANS

Toxoplasma gondii

Life cycle

The phylum Apicomplexa is divided into four classes, the Gregarinea, Haemosporidea, Piroplasmea and Coccidea, which together comprise over 5,000 named species of protozoan parasites [1]. The coccidea are the largest class (~1,500 species) and include various pathogens of man and animals [*Eimeria*, *Sarcocystis*, *Neospora*, *Cryptosporidium*, *Cyclospora* and *Toxoplasma gondii*]. *T. gondii*, the subject of this thesis, is capable of infecting an unusually broad range of hosts and many different cell types. *Toxoplasma* is facultatively heteroxenous (two host life cycle) and causes one of the most common parasitic zoonoses in the world (Fig. 1-1) [2-3]. There are three infectious stages in the life cycle of *T. gondii;* sporozoites, tachyzoites and bradyzoites. *T. gondii* is unique among heteroxenous coccidians in that all three of these parasite forms are infectious to both intermediate and definitive hosts. Three routes are responsible for *Toxoplasma* infection: 1) horizontal transmission by oral ingestion of oocysts (sporozoites) from the environment, 2) horizontal transmission of tissue cysts (bradyzoites) by oral ingestion of raw or undercooked meat, 3) vertical transmission of

tachyzoites via the placenta of infected mothers [3-4]. It has also been reported that tachyzoites may be transmitted through milk from mother to offspring [3].

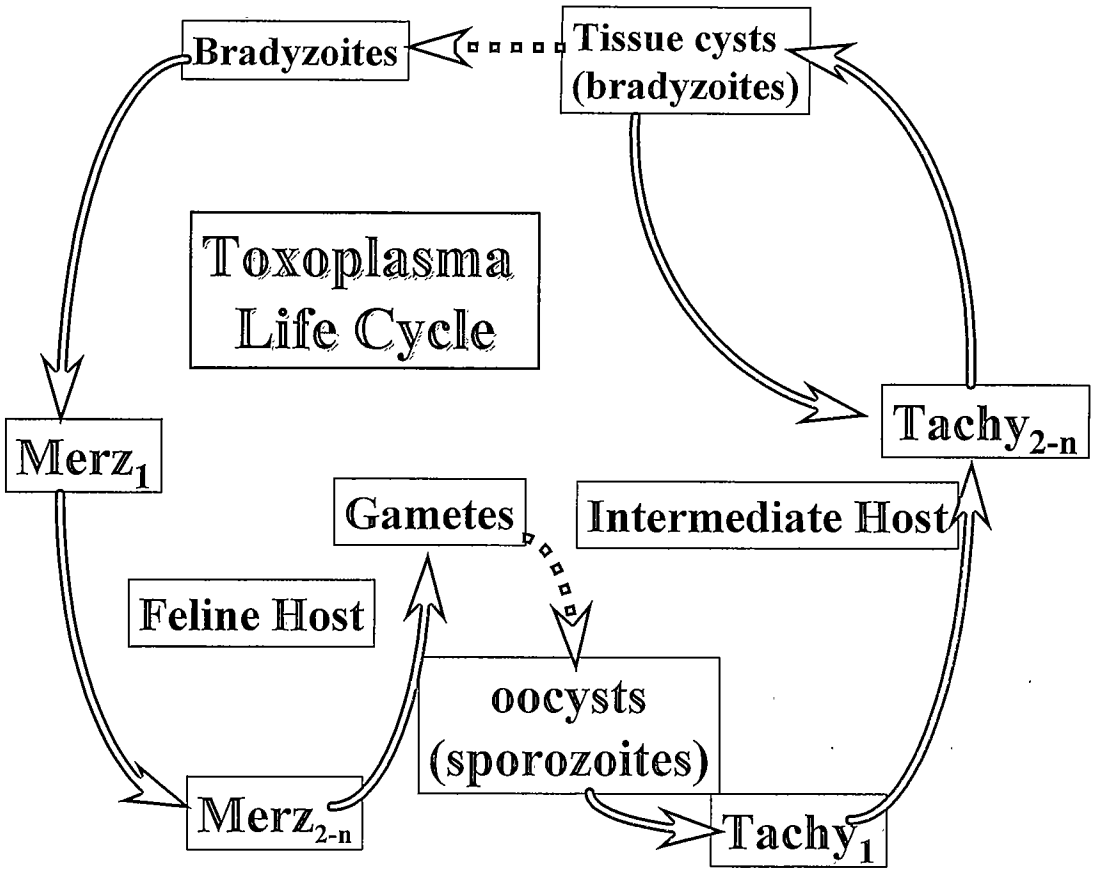

Figure 1-1: Life cycle of *Toxoplasma gondii*.

As with other coccidians, the *T. gondii* oocyst is the environmentally protective housing for the sporozoite [2]. When oocysts are ingested by an intermediate host, sporozoites excyst and actively penetrate cells of the intestinal tract where they differentiate into replicating tachyzoites. Tachyzoites multiply rapidly by repeated rounds of endodyogeny and will ultimately develop into bradyzoites contained within a protective tissue cyst. Tissue cysts are the end-stage of the intermediate life-cycle and

are capable of persistence for the life of the host. It is postulated that tissue cysts break down periodically and bradyzoites differentiate back into tachyzoites, which renews the pathogenic cycle (recrudescence) and is the basis of chronic disease in immunocompromised individuals [3]. Alternatively, bradyzoites are released from tissue cysts when ingested by a new animal host and differentiate into a tachyzoite to begin the intermediate life cycle. The location and number of tissue cysts in animals differ with respect to host and *T. gondii* strain [5]. In mice and rats, tissue cysts were more prevalent in the brain [5] whereas higher mammals present more cysts in muscular tissues [5].

Within the feline host, bradyzoite development follows the definitive life-cycle [2]. Bradyzoite invasion of feline enterocytes results in differentiation into merozoites that replicate for several cycles prior to forming gametocytes. The ensuing processes of gamogony and oocyst formation take place within the epithelium of the small intestine. After fertilization of a macrogametocyte by a microgamete, the zygote forms within an oocyst that is passed into the intestinal lumen and shed in the feces. The zygotes (the only diploid stage) in the oocyst undergo meiosis to form eight haploid sporozoites, which are subcompartmentalized into two groups of four, each group is contained in a sporocyst. Sporozoites and tachyzoites ingested by a feline must first develop into bradyzoites prior to initiation of the definitive life cycle. Thus, the incubation period prior to oocyst shedding is characteristic of which developmental stage is present in the inoculum. Oocysts are shed 3 to 10 days after ingesting tissue cysts, >13 days after ingesting tachyzoites and >18 days after ingesting oocysts [3].

Disease and clinical relevance of *Toxoplasma* infections

A relatively small number of Apicomplexa species are responsible for the diseases of medical and veterinary significance (Table 1-1) [6-7]. Examples include *Plasmodium spp.,* which cause malaria, *Eimeria spp.*, which cause coccidiosis in animals, and *Toxoplasma gondii* which causes toxoplasmosis [2]. Toxoplasmosis in healthy, immunocompetent humans is common yet clinical presentation is often inapparent or misdiagnosed. Toxoplasmosis can be categorized into three states; acute, sub-acute and chronic. In the acute state (caused by tachyzoite parasitaemia), the most common symptoms are swollen lymph glands, associated fever headaches, and anemia, all of which are symptoms typically confused with influenza [2-3,8]. The sub-acute stage is characterized by formation of cysts in tissues such as liver, heart, brain and eyes [2-3,8]. The recrudescence of the tissue cyst (bradyzoite) back into the proliferative tachyzoite leads to a chronic infection. A number of factors influence the severity of disease symptoms including pathogen strain, susceptibility and age of the host, and the state of acquired immunity within the host.

ORGANISM	DISEASE	AFFLICTS
Toxoplasma	Toxoplasmosis	All warm-blooded animals, birds (30+ spp.)
Plasmodium	Malaria	Humans and Animals
Sarcocystis	Sarcocystosis	Humans, Mammals, Birds and Reptiles
Eimeria	Coccidiosis	Mammals and Birds
Cyclospora	Cyclosporiasis	Humans
Isospora	Isosporosis	Humans and Animals
Cryptosporidium	Cryptosporidiosis	Humans and Animals
Babesia	Babesiosis (redwater fever)	Cattle, other animals, man (rare)
Theileria	Theileriosis (East Coast Fever)	Cattle

Table 1-1: Apicomplexan diseases of medical and veterinary significance [6,7].

T. gondii infection within healthy individuals in the United States is thought to occur most commonly through the consumption of contaminated meat products, although the relative contribution of contaminated food versus environmental sources remains an open question [3-4]. Tissue cysts are present in edible tissues of approximately 30% of sheep and swine in the United States [2,9-11]. Outside of Europe and North America, the prevalence of infected animals increases to >50% (ex. in pigs) thereby leading to high rates of infection in some countries [3]. A higher percentage of food source infections have been found in populations of individuals within France, Panama and the continent of Africa where the seropositive rate can exceed 65% [4]. These findings support the hypothesis that crowded living conditions and cultural/eating habits contribute to the wide range of seropositivity among various populations [3].

Documented epidemics of oocyst infection have occurred raising concerns that environmental contact with oocysts is a threat to urban populations [12-14]. Two cases in North America have provided the foundation for this concern. At a riding stable in Atlanta Georgia 43% of individuals exposed to an oocyst source became seropositive [15]. In a case in Vancouver, Canada, 110 individuals presented with *T. gondii* infections as a result of contaminated water from a municipal water source [12]. In this local epidemic, it was estimated that several thousand individuals were exposed to contaminated water. High seropositive rates are seen in farm workers, gardeners [4], and a vegetarian life-style does not seem to minimize the risk of exposure [4] suggesting environmental transmission is a significant cause of toxoplasmosis.

The unborn and the immunocompromised are at significant risk for acquiring a *T. gondii* infection. The symptoms presented by these two groups include encephalitis, sepsis syndrome/shock, myocarditis, hepatitis and retinochoroiditis [3]. Congenital toxoplasmosis usually occurs when the mother acquires a primary *T. gondii* infection during pregnancy and may result in an abortion, neonatal death or fetal abnormalities. Vertical transmission occurs in mothers previously exposed to *T. gondii* who enter into an immunocompromised state during pregnancy either through the use of steroids, systemic lupus erythematosus or an HIV infection [3]. It has been suggested that in these women, the reactivation of a latent infection (recrudescence of the bradyzoite) resulted in transplacental transmission [3].

Children who survive a prenatal infection may have a significantly reduced quality of life with defects in vision, hearing, and central nervous system (CNS) deficiencies [3]. The frequency of prenatal infection varies from 1 to 100 per 10,000

births [3]. The risk of an interuterine infection increases during pregnancy but the most severe manifestations of toxoplasmosis occur when transmission comes at an early stage of pregnancy. In some states of the U.S.A. and various European countries (Austria, Italy, Denmark, Poland and France) programs have been initiated that are aimed at early detection of prenatal infection in neonates [3]. The prophylactic use of drugs on women of childbearing age is an unreasonable proposal. Through the implementation of effective screening programs, mothers can be treated with pyrimethamine and sulfadiazine providing an *in utero* therapy for the fetus. These drugs have been shown to decrease the severity of symptoms in infected children. More encouraging news comes from a study in which pregnant women who showed evidence of a recently acquired infection exhibited an ~40% decrease in the number of prenatal infections when given spiromycin during pregnancy [3]. Additionally, spiromycin has been shown to decrease the percentage of fetuses with severe disease or intrauterine death from 11 to 3% [3].

In immunocompromised individuals, either a primary infection or a previously acquired latent infection can lead to severe complications [3,16]. Encephalitis is the leading affliction in immunocompromised individuals infected with *T. gondii* [3,16]. In AIDS patients, the unique ability of bradyzoites and tachyzoites to interconvert is considered to be the underlying cause of *Toxoplasma*-induced encephalitis [16]. Consequently, AIDS patients are treated prophylactically with a combination of trimethoprin/sulfamethoxyzole which is often not well tolerated. Prophylactic treatment for this pathogen along with recent advances in antiretroviral therapies and immune reconstitution has reduced the incidence of CNS toxoplasmosis in AIDS patients [3,16].

Apicomplexan Biology

Genetics

Apicomplexan parasites have a wide range of genome sizes (8 Mb to >200 Mb). The genome of *Cryptosporidium parvum* is 8 Mb, *Plasmodium falciparum* 30 Mb, *Eimeria* spp. ~60 Mb and *Sarcocystis cruzi* may have the largest genome at 200 Mb [17]. *T. gondii* posseses two organellar genomes (apicoplast, ~35 kb and mitochondria, ~7 kb) and a nuclear genome estimated to be ~80 Mb (haploid) partitioned into at least 11 chromosomes ranging in size from 1.9 Mb to greater than 10 Mb [18]. Based on genome size and a rudimentary knowledge of intron/exon abundance, it is estimated that Apicomplexan genomes may contain as many as 10-15,000 genes [J. Ajioka, personal communication]. This is likely an overestimate, particularly for the small *Cryptosporidium* genome, although there appear to be few introns in this unusual member of the Apicomplexa [M. Abrahamsen personal communication]. *T. gondii* nuclear DNA has a 55% GC content as compared to *Plasmodium* spp., which have a 20% GC content [16]. Unlike other coccidian parasites, *T. gondii* codon usage is relatively unbiased [17].

Phylogenetic analysis indicates that three genotypic lineages of *T. gondii* account for most of the strains found in the world [21]. The RH strain (Type I) is the most extensively used strain for experimental and genetic manipulations [22]. Type I strains have an essentially identical genotype leading to the hypothesis that they are derived from a single clonal lineage [23]. Type I strains have a reduced ability to undergo the definitive life cycle in cats and are highly virulent in mice as opposed to Type II and III

strains which are comparatively avirulent but are capable of efficiently initiating the definitive life cycle in the feline. The laboratory strain ME49-Plk represents the Type II variant most often identified within HIV patients that present with acute *Toxoplasma*-encephalitis [21]. The Type III strain is most commonly found in livestock and is the second most common strain found in HIV patients. Interestingly, karyotype comparisons between the three major clonal lineages show very little chromosome size variation as compared to other Apicomplexa. The karyotype of RH strain, for example, has remained virtually unchanged in more than 50 years of culture [18,23-24]. T. gondii isolates can be divided into two virulence classes based on experiments in mice. The 50% lethal dose (LD_{50}) for most strains is dose dependent (requires 10^2-10^5 parasites) [25]. The acutely virulent Type I strains cause mortality at a very low parasite inoculum (LD_{50} <10^2) [25].

Three Apicomplexan genomes have been sequenced; *P. falciparum*, *C. parvum* and *Theileria parvum* [26-28]. The combined efforts of an EST project and a recently funded genome sequencing project have begun to provide resources for *T. gondii* [29-31]. The current *Toxoplasma* EST database includes ~3200 ESTs derived from sporozoite cDNA libraries (1262 unique), 17,000 tachyzoite ESTs representing ~6600 unique sequences and ~3300 ESTs obtained from bradyzoite cDNA libraries which represent 1289 unique sequences.

T. gondii has proven to be an important Apicomplexan model due to the relative ease of *in vitro* genetic manipulations in the tachyzoite stage. More than 50% of parasites express transiently after electroporation and non-homologous integration of DNA can occur in 1/20 viable parasites (RH strain) transfected using one of several selectable markers; hypoxanthine-xanthine-guanine phosphoribosyl transferase (HXGPRT),

chloramphenicol, pyrimethamine, or phleomycin [32-35]. *Toxoplasma* expression vectors with a variety of promoter strengths, fluorescent markers (CFP, YFP, GFP, RFP), epitope tags, and targeting sequences are now available [36]. Using fluorescent markers, proteins associated with the cytoskeleton [36], the nucleus [37], or targeted to specialized organelles including the plastid [36,38-39] have all been characterized. Antisense protocols have been used to study the functions of nucleoside triphosphate hydrolase [40] and HXGPRT [41]. Recently a rudimentary tetracycline-inducible system was described [42].

The high level of non-homologous integration in *Toxoplasma* allows for a large portion of the parasite genome to be marked [43]. Through genomic tagging by insertional mutagenesis, a gene can be identified whose inactivation is not lethal and for which a suitable selection screen is available [43-45]. Initial studies of gene function and expression rely on the use of cDNA sequences (typically <2kb) that typically incorporate into the genome by non-homologous recombination. Larger fragments of genomic DNA can switch the targeting from a non-homologous to homologous type of integration. Using genomic sequences >8kb, of which ~ 4 kb flank the selectable marker, has resulted in ~50% of integrations occurring by homologous recombination. Examples of homologous integrations generating gene replacements include: dihydrofolate-reductase (DHFR) [46], HXGPRT [47], bradyzoite antigen 1 [48], adenosine kinase [49], uracil phosporibosyl transferase [50], rhoptry protein 1 [33] and dense granule protein two (GRA2) [51]. Until recently, the major deficiency in the *Toxoplasma* genetic "tool-kit" was a robust forward genetic model for complementation. An episomal library containing *T. gondii* genomic fragments [52] was unsuccessful due to the high integration

rate. A new strategy has now been developed that combines phage recombination [53] with the high level of stable integration in the tachyzoite [See Chapter #5 and 54].

Cell Biology of Growth

Apicomplexan parasites undergo three types of nuclear/cellular division. Schizogony results when multiple nuclei are formed by alternating rounds of DNA synthesis (S) and mitosis (M) ((S-M-ND)n–C-G1) (representative organisms: *Eimeria callospermophilli* and *T. gondii* merozoites) [55, Speer unpublished observations]. Budding of daughter parasites (cytokinesis - C) is delayed until the last round of nuclear division. In endopolygeny ((S–M)n–ND/C–G1) (representative organisms: *Sarcocystis tenella* and *Plasmodium berghei*), multiple rounds of DNA replication occur in the absence of mitosis, thereby generating a single polyploid nucleus that subsequently undergoes multiple mitotic events in conjunction with concerted parasite budding [56-57]. Endodyogeny, the mode of division of the *T. gondii* tachyzoite, has long been considered a binary form of schizogony [58-59]. In endodyogeny (S-M/C-G1), DNA synthesis is followed by mitosis and parasite budding, which results in a process that is indistinguishable from the final cycle of schizogony.

Interestingly, the scale, if not the number, of schizogonous nuclear divisions appears to be predetermined in many of the Apicomplexa. For example, *Eimeria bovis* sporozoites invariantly produce very large schizonts (with >100,000 first-generation merozoites) [60], while sporozoites of *Cryptosporidium parvum* only form small schizonts that produce 6-8 merozoites [61]. In each case the relative size of the schizont

is predetermined and obligatory to further development. Thus, it is evident that growth control can directly affect the course of parasite development. The idea that growth control and development are linked was recently explored in *T. gondii*, and it was established that tachyzoites emerging from sporozoite-initiated infections undergo a rapid growth for 20 divisions, followed by a spontaneous shift to a slower growth rate that precedes differentiation into the bradyzoite [62]. This growth shift occurs at least 24 h prior to the expression of bradyzoite markers.

The structural features of parasite budding in *T. gondii* have been examined in detail [58] by electron microscopy. Budding is first recognized by division of the Golgi and by the appearance of conoid structures (apical complexes) in the tachyzoite cytoplasm. These structures appear prior to nuclear division and are almost always anterior to the nuclear envelope [63]. As budding continues, two inner membrane complexes emerge and extend posteriorly from each of the central apical complex structures in order to enclose their half of the mother cell organelles. Into each immature daughter parasite a divided nucleus migrates while the inner membrane complexes continue to expand. Ultimately, the daughter cells consume most of the mother cell, although they may remain joined posteriorly (rozetta) for several divisions.

Recently, the features of tachyzoite endodyogeny have been placed within the framework of the eukaryotic cell cycle. The tachyzoite cell cycle is unusual in that it is comprised primarily of a G1 and a bimodal S-phase [37,64]. Tachyzoite division can be partitioned into ~60% G1, ~30% S phase and ~10% G2+M phases [37,64]. A significant fraction of tachyzoites possess a 1.7-1.8 N DNA content, indicating that DNA synthesis may be unequal with ~20% of the genome replicating just prior to entering mitosis. This

cell cycle feature remains to be confirmed; however, it is noteworthy that gametocytes of *Toxoplasma* and *Plasmodium* spp. appear to pause or slow chromosome replication (1.7 N) prior to invasion of the next host cell where chromosome replication is completed [17, 65-66]. In this regard, the *Plasmodium* microgametocyte is remarkable, as chromosome replication is interrupted indefinitely until the gametocytes move into the insect host at the time of a blood meal. Whether this pause in DNA synthesis represents a novel cell cycle checkpoint remains to be determined.

The subsequent chapters describe work in *T. gondii* which has provided insight into the mechanisms involved in the linkage between growth and development. The hypothesis for chapters 2 and 4 is as follows: Proliferating cell nuclear antigen (PCNA) is an essential co-factor of DNA replication and repair in eukaryotes, and is present as a single gene. Apicomplexa have two PCNAs and we hypothesize that one PCNA is essential for DNA replication and the second PCNA functions in repair. The initial characterization of these two genes was reported in Guerini et al. [67] and appears as chapter 2 in this thesis. The work presented in chapter 3 begins with experiments that use TgPCNA1 and 2 as a marker for proliferation and this work is based on the hypothesis that a cell cycle switching mechanism is involved in differentiation. Further work in this chapter characterizes the recrudescent pathway. Chapter 5 describes work using a forward genetics approach [54] to complement a loss-of-function mutant in *Toxoplasma*. This work was performed to prove that a forward genetics approach to complementing temperature sensitive (*ts*) tachyzoite mutants was functional and that the Cyclin B pathway might play a role in the defect associated with *ts*11C9 [68].

References

1. Cox FEG. The evolutionary expansion of the Sporozoa. Int J Parasitol 1994;24(8):1301-1316.

2. Dubey JP, Beattie CP. Toxoplasmosis of Animals and Man. Boca Raton, Florida: CRC Press 1988.

3. Tenter AM, Heckeroth AR, Weiss LM. *Toxoplasma gondii*: from animals to humans. Int J Parasitol 2001;30:1217-1258.

4. Jones JL, Kruszon-Moran D, Wilson M, Mcquillan G, et al., *Toxoplasma gondii* Infection in the United States: Seroprevelance and Risk Factors. Am J Epidem 2001;154(4):357-365.

5. Dubey JP, Lindsay DS, Speer CA. Structures of *Toxoplasma gondii* tachyzoites, bradyzoites, and sporozoites and biology and development of tissue cysts. Clin Microbiol Rev 1998;11:267-299.

6. Peters W. and Gilles HM. A colour Atlas of Tropical Medicine and Parasitology. Wolfe Medical Publications Ltd. 1989.

7. Smyth JD. Introduction to Animal Parasitology. Cambridge University Press. 1994.

8. Weiss LM, Kim K. The development and biology of bradyzoites of *Toxoplasma gondii*. Front Biosci 2000;5:D391-405.

9. Fitzgerald PR. The significance of bovine coccidiosis as a disease in the United States. Bovine Practitioner 1975;10:28-32.

10. Malik MA, Dreesen DW, de la Cruz A. Toxoplasmosis in sheep in northeastern United States J Am Vet MEd Assoc 1990;196:263-5.

11. Gamble HR, Brady RC, Dubey JP. Prevelance of Toxoplasma gondii infection in domestic pigs in NEw England states. Vet Parasitol 1999;82:129-36.

12. Bowie WR, King AS, Werker DH, Isaac-Renton JL, Bell A, Eng SB, Marion SA. Outbreak of *Toxoplasma* associated with municipal drinking water. THE LANCET 1997;350:173-177.

13. Dubey JP. A review of toxoplasmosis in pigs. Vet Parasitol 1986;19:181-223.

14. Konishi E, Takahashi J. Some epidemiological aspects of *Toxoplasma* infections in a population of farmers in Japan. Intl J Epidemiol 1987;16:277-281.

15. Dubey JP, Sharma SP, Juranek DD, Sulzer AJ. Characterization of *Toxoplasma gondii* isolates from an outbreak of toxoplasmosis in Atlanta, Georgia. Am J Vet Res 1981;42:1007-10.

16. Luft BJ, Remington JS. Toxoplasmic encephalitis in AIDS. Clin Infect Dis 1992;15:211-222.

17. Cornelissen AWCA, Overdulve JP, Van Der Ploeg M. Determination of nuclear DNA of five Eucoccidian parasites, *Isospora* (*Toxoplasma*) *gondii, Sarcocystis cruzi, Eimeria tenella, E. acervulina and Plasmodium berghei*, with special reference to gamonto-genesis and meiosis in *I.* (*T.*) *gondii*. Parasitol 1984;88:531 553.

18. Sibley LD, LeBlanc AJ, Pfefferkorn ER, Boothroyd JC. Generation of a restriction fragment length polymorphism linkage map for *Toxoplasma gondii*. Genetics 1992;132:1003-1015.

19. Janse, CJ Chromosome size polymorphism and DNA rearrangements in *Plasmodium*. Parasitology Today 1993;(9):19-22.

20. Johnson AM. Comparison of dinucleotide frequency and codon usage in *Toxoplasma* and *Plasmodium*: evolutionary implications. J Mol Evol 1990;30(4):383-387.

21. Howe DK, Sibley LD. *Toxoplasma gondii* comprises three clonal lineages: correlation of parasite genotype with human disease. J Infect Dis 1995;172:1561-1566.

22. Roos DS, Donald RGK, Morrissette NS, Moulton ALC. Molecular tools for genetic dissection of the protozoan parasite *Toxoplasma gondii*. Meth Cell Biol 1995;45:25-61.

23. Sibley LD, Boothroyd JC. Virulent strains of *Toxoplasma gondii* comprise a single clonal lineage. Nature 1992b;359:82-85.

24. Sibley LD, Boothroyd JC. Construction of a molecular karyotype for *Toxoplasma gondii*. Mol Biochem Parasitol 1992a;51:291-300.

25. Sibley LD, Howe DK. Genetic basis of pathogenicity in Toxoplasmosis. Curr Top Microbiol Immun 1996;315:3-15.

26. Craig AG, Waters AP, Ridley RG. Malaria genome project task force: a post-genomic agenda for functional analysis. Parasitol Today 1999;15(6):211-214.

27. Roos DS, Crawford MJ, Donald RG, Fraunholz M et al. Mining the *Plasmodium* genome database to define organellar function:what does the apicoplast do? Philos Trans R Soc Lond B Biol Sci. 2002;357(1417):35-46.

28. Prichard R, Tait A. The role of molecular biology in veterinary parasitology. Vet Parasitol 2001;98(1-3):169-194.

29. Wan KL, Blackwell JM, Ajioka JW. *Toxoplasma gondii* expressed sequence tags: insight into tachyzoite gene expression. Mol Biochem Parasitol 1996;75(2):179-186.

30. Ajioka J, Boothroyd JC, Brunk BP, Hehl A, Hillier L, Manger ID, Overton GC, Marra M, Roos D, Wan KL, Waterston R, Sibley LD. Sequencing of ESTs from the protozoan parasite *Toxoplasma gondii*: efficient identification of genes and identification of phylogenetically restricted sequences of the Apicomplexa. Genome Res 1998; 8:18-28.

31. Manger ID, Hehl A, Parmley S, Sibley LD, Marra M, Hillier L, Waterston R, Boothroyd JC. Expressed Sequence Tag Analysis of the Bradyzoite Stage of *Toxoplasma gondii*: Identification of Developmentally Regulated Genes. Infect Immun 1998;66(4):1632-1637.

32. Donald RG, Carter D, Ullman B, Roos DS. Insertional tagging, cloning, and expression of the *Toxoplasma gondii* hypoxanthine-xanthine-guanine phosphoribosyl transferase gene. Use as a selectable marker for stable transformation. J Biol Chem. 1996;271(24):14010-14019.

33. Kim K, Soldati D, Boothroyd JC. Gene replacement in *Toxoplasma gondii* with chloramphenicol acetyltransferase as selectable marker. Science 1993;262(5135):911-14.

34. Donald RG, Roos DS. Stable molecular transformation of *Toxoplasma gondii*: a selectable dihydrofolate reductase-thymidylate synthase marker based on drug resistance mutations in malaria. PNAS USA 1993;90(24):11703-11707.

35. Soldati D, Kim K, Kampmeier J, Dubremetz JF, Boothroyd JC. Complementation of a *Toxoplasma gondii* ROP-1 knock-out mutant using phleomycin selection. Mol Biochem Parasitol 1995;74(1):87-97.

36. Striepen B, He CY, Matrajt M, Soldati D, Roos DS. Expression, selection and organellar targeting of the green fluorescent protein in *Toxoplasma gondii*. Molec Biochem Parasitol 1998;92:325-338.

37. Radke JR, Striepen BS, Guerini MN, Jerome ME Roos DS, White MW. Defining the cell cycle of the tachyzoite stage of *Toxoplasma gondii*. Mol Biochem Parasitol 2001;115:165-175.

38. Waller RF, Keeling PJ, Donald RG, Striepen B, Handman E, Lang-Unnasch N, Cowman AF, Besra GS, Roos DS, McFadden GI. Nuclear-encoded proteins target to the plastid in *Toxoplasma gondii* and *Plasmodium falciparum*. Proc Natl Acad Sci USA 1998;95(21):12352-7.

39. Roos DS, Crawford MJ, Donald RGK, Kissinger JC, Klimczak LJ, Streipen B. Origin, targeting, and function of the apicomplexan plastid. Curr Opin Micro 1999;2:426-432.

40. Nakaar V, Samuel BU, Ngo EO, Joiner KA. Targeted reduction of nucleoside triphosphate hydrolase by antisense RNA inhibits *Toxoplasma gondii* proliferation. J Biol Chem 1999;274(8):5083-7.

41. Nakaar V, Ngo EO, Joiner KA. Selection based on the expression of antisense hypoxanthine-xanthine-guanine phosphoribosyltransferase RNA in *Toxoplasma gondii*. Mol Biochem Parasitol 2000;110(1):43-51.

42. Meissner M, Brecht S, Bujard H, Soldati D. Modulation of myosin A expression by a newly established tetracycline repressor-based inducible system in *Toxoplasma gondii*. Nucleic Acids Res. 2001;29(22):E115.

43. Roos DS, Sullivan WJ, Striepen B, Bohne W, Donald RG. Tagging genes and trapping promoters in *Toxoplasma gondii* by insertional mutagenesis. Methods 1997;13(2)112-122.

44. Knoll LJ, Boothroyd JC. Isolation of developmentally regulated genes from *Toxoplasma gondii* by a gene trap with the positive and negative selectable marker hypoxanthine-xanthine-guanine phosphoribosyltransferase. Mol Cell Biol 1998;18(2):807-14.

45. Donald RG, Roos DS. Insertional mutagenesis and marker rescue in a protozoan parasite: cloning of the uracil phosphoribosyltransferase locus from *Toxoplasma gondii*. Proc Natl Acad Sci USA 1995;92(12):5749-53.

46. Donald RG, Roos DS. Homologous recombination and gene replacement at the dihydrofolate reductase-thymidylate synthase locus of *Toxoplasma gondii*. Mol Biochem Parasitol. 1994;63(2):243-253.

47. Donald RGK, Roos DS. Gene knock-outs and allelic replacements in *Toxoplasma gondii*: HXGPRT as a selectable marker for hit-and-run mutagenesis. Molec Biochem Parasitol 1998;91:295-305.

48. Bohne W, Hunter CA, White MW, Fergusson DJ. Targeted disruption of the bradyzoite-specific gene BAG-1 does not prevent tissue cyst formation in *Toxoplasma gondii*. Mol Biochem Parasitol 1998;92(2):291-301.

49. Sullivan WJ, Chiang C-W, Wilson C, Naguib FNM. Insertional tagging of at least two loci associatede with resistance to adenine arabinoside in *Toxoplasma gondii*, and cloning of the adenosine kinase locus. Mol Biochem Parasitol 1999;103(1):1-14.

50. Donald RG, Roos DS. Gene knock-outs and allelic replacements in *Toxoplasma gondii*: HXGPRT as a selectable marker for hit-and-run mutagenesis. Mol Biochem Parasitol 1998;91(2):296-305.

51. Mercier C, Howe DK, Mordue D, Lingnau M, Sibley LD. Targeted disruption of the GRA2 locus in *Toxoplasma gondii* decreases acute virulence in mice. Infect Immun 1998;66(9):4176-4182.

52. Black MW, Boothroyd JC. Development of a stable episomal shuttle vector for *Toxoplasma gondii*. J Biol Chem. 1998;273(7):3972-9.

53. Hartley JL, Temple GF, Brasch MA. DNA cloning using in vitro site-specific recombination. Genome Res. 2000;10(11):1788-95.

54. Striepen B, White MW, Li C, Guerini MN. Genetic Complementation in Apicomplexan Parasites. Proc Natl Acad Sci USA 2002;(In press).

55. Roberts WL, Hammond DM, Anderson LC, Speer CA. Ultrastructural study of schizogony in *Eimeria callospermophili*. J Protozool 1970;17:584-592.

56. Speer CA, Dubey JP An ultrastructural study of first- and second-generation merogony in the coccidian *Sarcocystis tenella*. J Protozool 1981;28:424-431.

57. Canning EU, Sinden RE. The organization of the ookinete and observations on nuclear division in oocysts in *Plasmodium berghei*. Parasitol 1973;67:29-40.

58. Sheffield HG, Melton ML. The fine structure and reproduction of *Toxoplasma gondii*. J Parasitol 1968;54(2):209-226.

59. Ogino N, Yoneda C. The fine structure and Mode of Division of *Toxoplasma gondii*. Arch Opthal 1966;75:218-227.

60. Reduker DW, Speer CA. Effect of sporozoite inoculum size on *in vitro* production of first generation merozoites of *Eimeria bovis*. J. Parasitol 1987;73:427-430.

61. Fayer R, Speer CA, Dubey JP. *Cryptosporidium* and Cryptosporidiosis. Boca Raton, Florida: CRC Press, Inc. 1997.

62. Jerome ME, Radke JR, BohneW, Roos DS, White MW. *Toxoplasma Gondii* Bradyzoites Form Spontaneously during Sporozoite-Initiated Development. Infect Immun 1998;66(10):4838-4844.

63. Striepen B, Crawford MJ, Shaw MK, Tilney LG, Seeber F, Roos DS. The plastid of *Toxoplasma gondii* is divided by association with the centrosomes. J Cell Biol 2000;151(6):1-13.

64. Radke J, White MW. A cell cycle model for the tachyzoite of *Toxoplasma gondii* using the Herpes simplex virus thymidine kinase. Mol Biochem Parasitol 1998;95:237-247.

65. Janse, C. J., Ponnudurai, T., Lensen, A. H. W., Meuwissen, J. H. E. T., van der Ploeg, M., and Overdulve, J. P. DNA synthesis in gametocytes of *Plasmodium falciparum*. Parasitol 1988;96:1-7.

66. Janse, C. J., van der Klooster, P. F. J., van der Kaay, H. J., van der Ploeg, M., and Overdulve, P. DNA synthesis in *Plasmodium berghei* during asexual and sexual development. Mol Biochem Parasitol 1986;20:173-182.

67. Guerini MN, Que X, Reed SL, White MW. Two genes encoding unique proliferating-cell-nuclear-antigens are expressed in *Toxoplasma gondii*. Mol Biochem Parasitol 2000;109(2):121-131.

68. Radke JR, Guerini MN, White MW. *Toxoplasma gondii*: Characterization of temperature-sensitive tachyzoite cell cycle mutants. Exp Parasitol 2000;96:168-177.

CHAPTER 2

TWO GENES ENCODING UNIQUE PROLIFERATING-CELL-NUCLEAR-ANTIGENS ARE EXPRESSED IN *TOXOPLASMA GONDII.*

Introduction

The haploid genome of *Toxoplasma gondii* consists of 80 mb partitioned between 11 chromosomes [1]. Little is understood about *T. gondii* chromosome structure or the mechanisms of chromosome replication, although a low-resolution genetic map [2-3] based, in part, on expressed-sequence-tags has been generated for this parasite [4]. What is known about *T. gondii* division derives primarily from decades old ultrastructural observations [5]. Members of the phylum Apicomplexa, to which *T. gondii* belongs, replicate by simple binary division (endodyogeny) or by multinuclear processes (schizogony) that either involve multiple rounds of S and M phase prior to cytokinesis or the synthesis of polyploid chromatin followed by a single, multifocal mitosis and cytokinesis [6]. Schizogonous mechanisms appear to govern *T. gondii* multiplication in its definitive feline host, whereas in the intermediate host, asexual replication of the tachyzoite is exclusively by endodyogeny [6]. Rapid tachyzoite division is closely associated with virulence, which parallels reports that virulent isolates have elevated DNA polymerase activity [7]. This observation is potentially important to understanding acute disease caused by Type-I virulent strains [3]; however, further work is needed in

order to identify specific components of the DNA replication machinery that may be linked to virulence.

Proliferating Cell Nuclear Antigen (PCNA) is a ubiquitous co-factor of eukaryotic DNA synthesis and repair [8-9]. Attempts to generate ▲PCNA diploids in yeast have been unsuccessful, demonstrating this protein is essential for cell survival and implying a critical role in DNA replication [10-11]. PCNA is thought to specifically function by increasing the processivity of DNA polymerases δ and ε and in this way possesses a similar function to the β-subunit of the *E. coli* DNA polymerase III holoenzyme and the product of gene-45 of bacteriophage-T4 [12]. Animal and yeast PCNAs are relatively small proteins (~30 kDa) that are thought to function as homotrimeric ring structures. Assembly of the PCNA ring on chromosomes appears to be initiated by the binding of replication factor-C, which then recruits PCNA and polymerase δ to form an active replication complex [13-15].

Dramatic increases in PCNA levels have been shown to occur as animal cells enter S phase following a period of growth arrest [16]. Although originally thought to be S-phase specific, it is now accepted that PCNA levels marginally increase (~2-fold) in cycling animal cells and is more accurately considered an indicator of cell cycle entry from a G_0 state [8,16]. In *Plasmodium falciparum,* PCNA expression is tightly regulated during intraerythrocytic development [17]. Early, uninucleate ring stages (G1 phase) contain little, if any, PCNA mRNA or protein. PCNA induction is first detected in the late ring stage and is maximally expressed in trophozoites. This progression correlates with the onset of parasite DNA replication in the intraerythrocytic cycle, and thus, PCNA expression is also observed in schizonts undergoing mitosis and cytokinesis [17-18].

These studies illustrate the value of PCNA as a marker to delineate the periods of the cell cycle during the developmental transitions of other apicomplexan parasites. In this chapter, we describe the cloning and expression of two unique PCNA genes in *T. gondii*.

Materials and Methods

Cell culture and parasite growth

Human foreskin fibroblasts (HFF) were grown in Dulbecco's Modified Eagle Medium (Gibco BRL, Grand Island NY) supplemented with either 10% (v/v) newborn calf serum or fetal bovine serum (Hyclone Laboratories Inc., Logan UT). *T. gondii* tachyzoites of three strains: RH (Type I), ME49-PLK (Type II) and VEG (Type III) were maintained by serial passage in HFF cells according to standard methods [19-21]. Tachyzoites were purified from host cell monolayers by filtration through 3.0 μM Nucleopore filters (Costar, Cambridge, MA).

PCNA cDNA Cloning

Initial clones were obtained for TgPCNA1 by using reverse-transcription/PCR and degenerate oligonucleotide primers to conserved N-terminal (-Y/FRCDR-) and C-terminal (Y/FLAPK) PCNA sequences. Preliminary TgPCNA2 sequence information was discovered by examination of the *T. gondii* EST database (TgESTzy03b07.r1) [4,22]. Complete sequences for each of the TgPCNAs were then isolated by screening a λ ZAPII

RH strain cDNA library (NIH, AIDS reagent #1896) using [^{32}P]-labeled TgPCNA specific probes. Full-length cDNA clones for *T. gondii* PCNA1 (TgPCNA1 Accession #AF242301) and PCNA2 (TgPCNA2 Accession #AF242302) were sequenced and deposited into GenBank™.

Based on sequence comparisons, a single divergent region in the 3' end of each TgPCNA (~27% nt homology and ~15% identity) was identified and gene-specific probes to this region were generated by PCR. The TgPCNA1 specific probe corresponds to amino acids 174 through 284 (~332 bp) and was cloned into pBSK+ after PCR using primers (5'-CGCGGATCCCTCAAGGAGACCTCGGAGTCGG-3') and (5'-CGCGG-ATCCTTTCACGTGGCCGATGCACGAGCG-3'). The TgPCNA2 probe encompasses amino acids 171 through 274 (~308 bp) and was PCR amplified for cloning using primers (5'-CCGGAATTCAGACCCACATGCAACTCTCTGCGC-3') and (5'-CCGGAATTCC-AGCGTGCTCCGCGATTGAGG-3').

Phylogenetic Analysis

The putative TgPCNA1 and 2 coding regions were aligned with protein sequences representative of the various eukaryotic PCNAs using the Clustal W program and default parameter values [23] with some manual refinements. Phylogenetic trees were generated using PHYLIP (Phylogeny Inference Package v3.5c) [24] with bootstrap analyses (100 replicates) processed through a distance matrix (PAM-350), analyzed by neighbor-joining methods, and the results compiled into a consensus tree. Accession numbers: *Homo sapiens*, NP 002583; *Mus musculus*, P17918; *Sarcophaga crassipalis*, O16852;

Drosophila melanogaster, P17917; *Zea mays*, AAD10528; *Nicotiana tabacum*, AAD19905; *Schizosaccharomyces pombe*, CAB38513; *Saccharomyces cerevisiae*, P15873; *P. falciparum* [PfPCNA1] CAA48673; *P. falciparum* [(PfPCNA2) Contig id 13124]; *Cryptosporidium parvum* [(CpPCNA1) Contig id 1079]; *C. parvum* [(CpPCNA2) Contig id 1123].

Southern and Northern Blot Analysis

T. gondii RH genomic DNA was isolated as previously described [25], digested with restriction enzymes *Bgl*II and *Eco*RI, electrophoresed through a 1% agarose gel and transferred to nitrocellulose. Hybridization of duplicate blots was performed at 42°C for 16 h in a solution containing 50% formamide and 6 X SSC using [^{32}P]-labeled inserts specific for each TgPCNA gene (see above). Following hybridization, nitrocellulose blots were washed three times in 2 X SSC containing 0.1% SDS at room temperature (10 min each) and then twice in 0.1 X SSC containing 0.1% SDS at 42°C (30 min each). Blots were exposed to x-ray film at -80°C.

Total RNA was prepared from RH, ME49-PLK, and VEG strain tachyzoites by TRIzol (Gibco-BRL, Grand Island NY) extraction and analyzed by Northern blot. Briefly, equal amounts of total RNA (4.5 μg) for each strain were loaded into duplicate lanes, separated on a 1.2% (w/v) formaldehyde-agarose gel and transferred to nitrocellulose. In the Northern blot hybridization experiment, the two probes had equal specific activities (TgPCNA1-1.67 x 10^8 cpm/μg DNA and TgPCNA2-1.61 x 10^8 cpm/μg DNA) as determined following purification of the labeled probes using ELUTIP

minicolumns (Schleicher and Schuell, Keene, NH). Hybridization and washes were completed as described above. To normalize the level of TgPCNA mRNA species within the blots, a *T. gondii* specific 18S rRNA oligonucleotide probe (5'-AGACCGAAGTC-AACGCGACC-3') [26] was 5'-end [^{32}P]-labeled (8 x 10^7 cpm/μg DNA) and used to reprobe the blots after stripping the previous probe in boiling water. Blots were exposed to x-ray film at -80°C and mRNA expression levels were quantified using a Bio-Rad Molecular FX Imager and the Quantity One software package (Ver 4, Bio-RAD, Hercules CA).

Production of Recombinant Protein and Antibody Reagents

The coding regions for TgPCNA1 and 2 were cloned into the *Sph*I and *Hind*III sites of the pQE-30 (Type I) plasmid vector (Qiagen, Chatsworth CA) and transformed into the expression bacteria M15[pREP4]. The TgPCNA1 coding sequence was amplified from the cDNA insert using the following primers (5'-ACATGCATGCATGTTGGAAGCCAAGCTCCAG-3') and (5'-CCCAAGCTT-CTCATCCATCATAGAGTCGTC-3'). TgPCNA 2 coding region was amplified from cDNA inserts using (5'-ACATGCATGCATGTTTGAGTGCACGATCGAGGGG –3') and (5'-CCCAAGCTTCTCTTCGTCGTCCTCTATTCTC-3'). The pQE-30 vector added six adjacent histidine residues to the N terminus (6xHis-tag) and allowed the recombinant proteins to be purified (using native conditions) to virtual homogeneity in one step using nickel-chelate affinity chromatography, as described by the manufacturer. Immune serum for each purified TgPCNA protein was prepared by immunizing mice

(BALB/c) 3 times intraperitoneally at 2-week intervals with 25 μg of purified recombinant protein emulsified in Hunter's Titermax® adjuvant (Sigma, St. Louis MO).

SDS-PAGE and Western blot analysis

Tachyzoites from three genotypic strains (RH, ME49-PLK and VEG) were lysed using M-PER Mammalian Protein Extraction Reagent (Pierce, Rockford, IL) containing 10 μg/ml each of antipain, leupeptin, chymostatin, pepstatin A, phenylmethylsulfonylfluoride and phenanthroline (Sigma, St. Louis MO). Aliquots equivalent to 15 X 10^6 tachyzoites were subjected to 12% SDS-PAGE under reducing conditions and transferred to nitrocellulose. Following transfer, the blots were blocked with 10% horse serum and then incubated overnight with anti-TgPCNA1 or 2 mouse polyclonal sera (1:2500). Antigen detection was accomplished by incubating blots with alkaline phosphatase-conjugated anti-mouse IgG (Promega, Madison WIS) diluted 1:7,500, followed by development in nitroblue tetrazolium and 5-bromo-4-chloro-3-indolylphosphate [27].

Results

Cloning and sequence comparison of the PCNA genes in *T. gondii*

Analysis of EST database entries along with conventional cDNA strategies identified two unique PCNA cDNAs in *T. gondii*, designated TgPCNA1 and TgPCNA2.

The 951 bp open reading frame of TgPCNA1 predicts a protein of 316 amino acids with a predicted molecular weight of 34,476 daltons. The TgPCNA2 clone contains a smaller open reading frame of 864 bp encoding a protein of 261 amino acids and a predicted molecular weight of 32,263 daltons. Consistent with all known eukaryotic PCNAs, the TgPCNA sequences contain basic helix-loop-helix DNA binding motifs (Fig. 2-1) that demonstrate >50% similarity to the equivalent region in human PCNA [8]. Other conserved motifs include the polymerase-δ and p21 putative binding sites (D-SHV-, Fig. 2-1) as well as the C-terminal sequences (-F/YLAP, Fig. 2-1) that appear essential for proper folding [28]. PfPCNA1 contains 10 and PfPCNA2 contains 9 additional C-terminal amino acids while *T. gondii* PCNA1 and 2 contain C-terminal insertions of 53 and 28 amino acids, respectively.

Southern analysis of *T. gondii* DNA with TgPCNA1- and 2-specific-probes shows a different hybridization pattern, confirming the existence of two unique PCNA genes (Fig. 2-2). A search of the *P. falciparum* genome sequence data (The Sanger Centre, Cambridge UK) also revealed the existence of two distinct PCNA genes. PfPCNA1 was found in sequence data from chromosome thirteen and is identical to the PCNA gene previously described by Kilbey *et al.* (1993). A second putative PCNA gene (designated PfPCNA2) was found in contig #13124 (The Sanger Centre) from chromosome twelve. TgPCNA1 and PfPCNA1 share the highest amino acid identity at 49%, compared to 38% identity for TgPCNA2 and PfPCNA2. Comparison of TgPCNA1 and CpPCNA1 demonstrated 42% identity, whereas the identities for TgPCNA2 and CpPCNA2 are 32%. Interestingly, intraspecies PCNAs share only 27-30% identity.

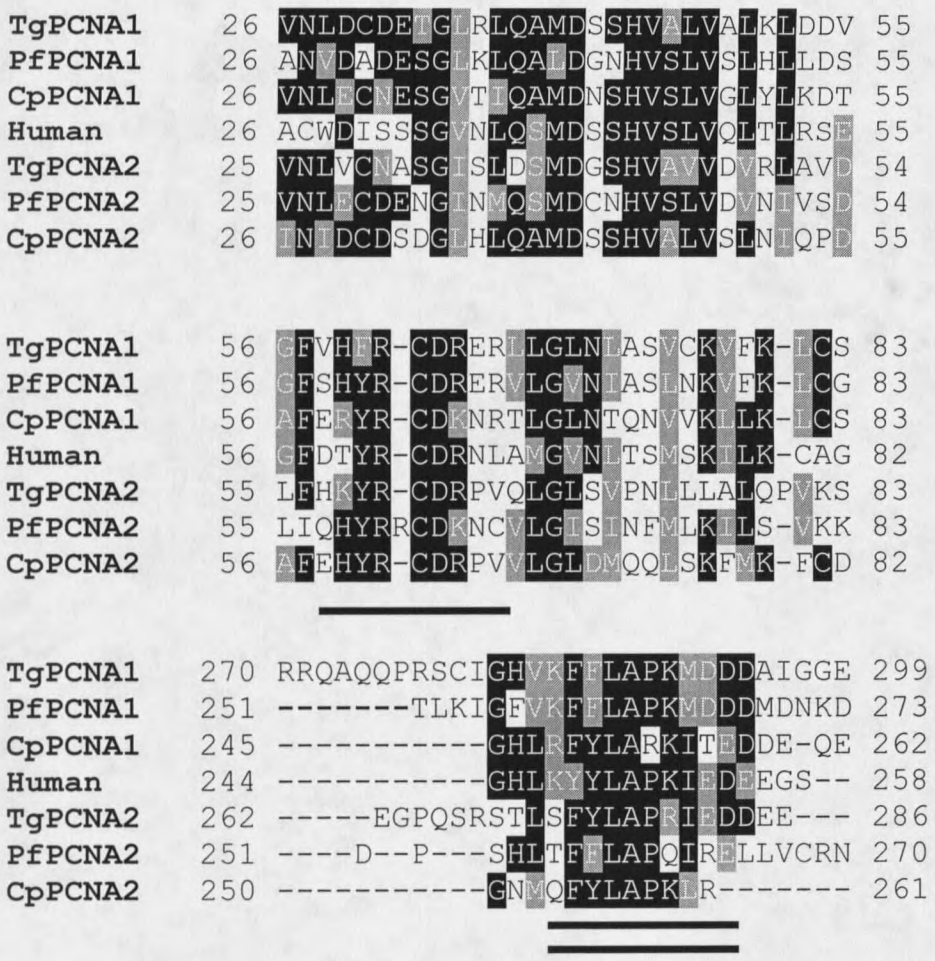

Figure 2-1. Amino acid alignments of the putative functional domains of two unique classes of PCNAs found in *Toxoplasma gondii*, *Plasmodium falciparum* and *Cryptosporidium parvum* compared to human PCNA. Conservation of amino acid sequences found in all PCNA sequences is illustrated by the DNA binding domain (aa 61-64 underlined) consisting of a basic helix-loop-helix sequence (-RCDR-). Motifs involved in polymerase-δ and p21 putative binding (D-SHV-) as well as the C-terminal sequence (-F/YLAP-, double underline) essential for proper folding are also found in the apicomplexan PCNAs. Note that PCNAs from each class are more similar than each pair of PCNAs from a single Apicomplexan. Black squares represent identical amino acids and gray represents conserved residues.

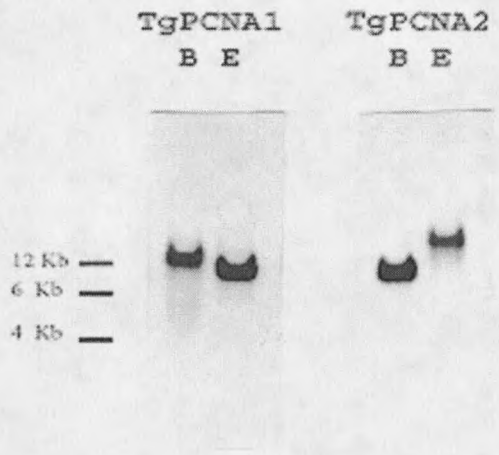

Figure 2-2. Southern analysis of *T. gondii* RH strain genomic DNA hybridized with TgPCNA1- and 2-specific probes. The hybridization pattern indicates the presence of two unique PCNA genes. DNA was digested with either *Bgl II* (lanes 1 and 3) or *Eco R1* (lanes 2 and 4). Lanes 1 and 2 were hybridized with the TgPCNA1 specific probe and lanes 3 and 4 were hybridized with the TgPCNA2 probe. Molecular mass markers (kb) are indicated to the left of the figure.

Phylogenetic analysis of Apicomplexan PCNA sequences

Distinct lineages within the eukaryotic PCNA family of proteins emerge on the basis of taxonomic assignment at the phylum level (Fig. 2-3). The grouping of humans and mice represents the phylum chordata while *Drospohila* and *Sarcophaga* represent the arthropoda. *Zea* and *Nicotiana* represent streptophyta and the two yeast organisms from the phylum ascomycota reside independent of any other group. *Toxoplasma*, *Plasmodium* and *Cryptosporidium* PCNAs group together representing the Apicomplexa. Although together, the apicomplexan sequences maintain an independent segregation between PCNA 1 and 2 (Fig. 2-3).

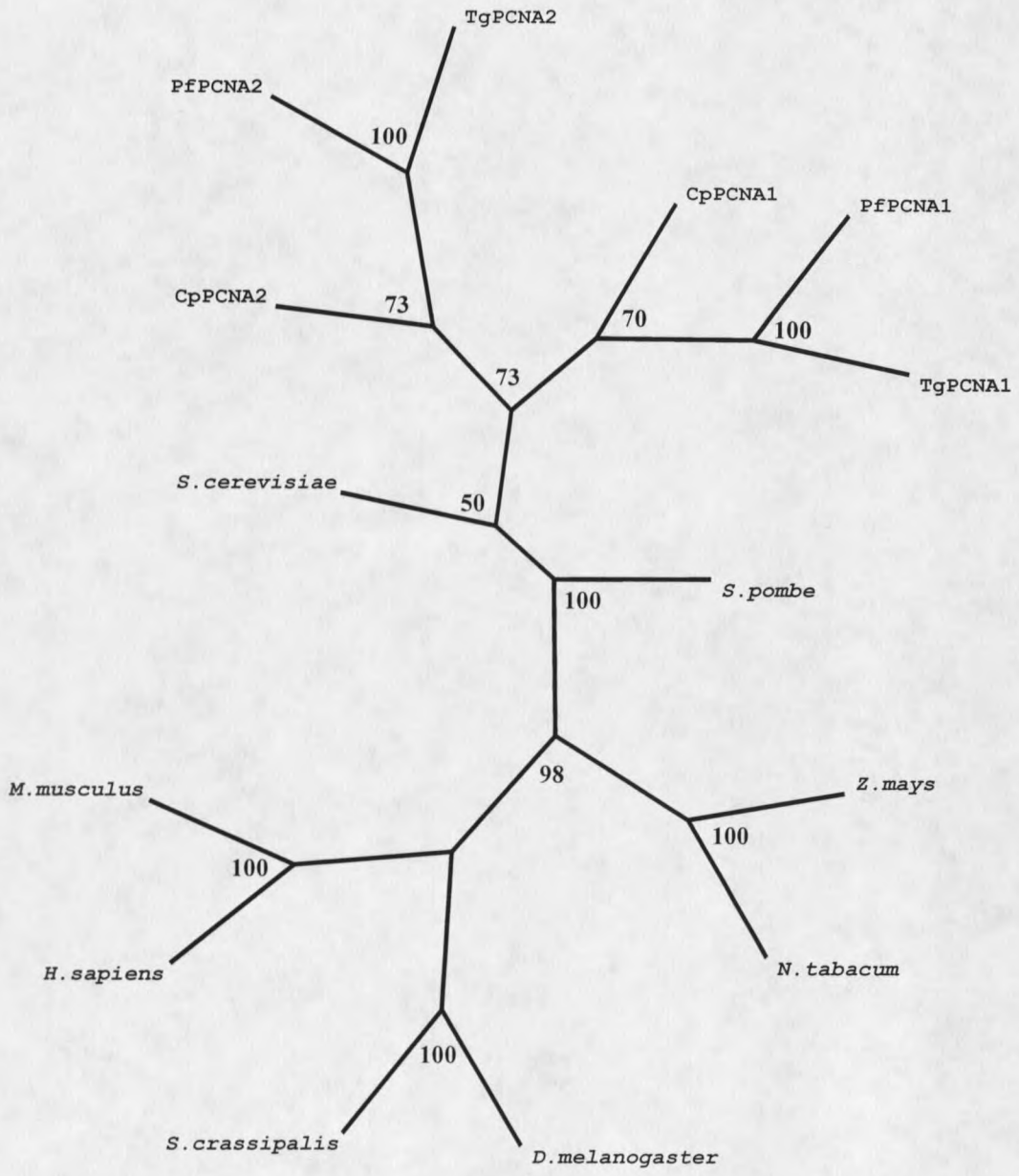

Figure 2-3. Consensus tree of Apicomplexa and representative eukaryotic PCNAs. Numbers along the branches represent the frequency of that group occurring in 100 bootstrap replicates. Lineages within the eukaryotic PCNA family of proteins emerge on the basis of taxonomic assignment. All six apicomplexan PCNAs group together, but the PCNA1 and 2 sequences segregate at the interspecies level.

TgPCNA1 and 2 mRNA expression

Previous molecular characterization of two nucleoside triphosphate hydrolase genes in *T. gondii* revealed the presence of two isoforms whose expression was strain specific [29]. Because TgPCNA cDNAs were identified from a single isolate (RH strain), we examined the expression of PCNA mRNA in tachyzoite isolates representative of the three genotypic classes (RH, ME49-PLK, and VEG). In Figure 2-4, duplicate Northern blots were hybridized with probes specific for each TgPCNA gene. TgPCNA 1 and 2 mRNAs were expressed in all three tachyzoite strains (Fig. 2-4 inset A). The probe specific for TgPCNA1 hybridized to multiple mRNA species. In all three strains, the largest species was ~3.6 kb, based on a comparison with 28S rRNA (Fig. 2-4 inset, upper arrow), while a second species (~2.2 kb) migrated a little slower than the 18S-like rRNA (Fig. 2-4 inset, lower arrow) [30-31]. A third mRNA species appeared in the Type-III (VEG) strain and was ~1.9 kb. The second TgPCNA1 mRNA species was greatly diminished in the Type-II strain (ME49-PLK) examined here. The basis for multiple PCNA1 mRNA species was not investigated. A single mRNA species of ~2.8 kb was detected by the TgPCNA2 probe (Fig. 2-4 inset A). Following normalization for equal RNA loading with a *T. gondii*-specific 18S rRNA probe, the combined expression of all forms of TgPCNA1 was found to be four to seven fold higher in all three tachyzoite strains, when compared to the levels of TgPCNA2 mRNA (Fig. 2-4 graph).

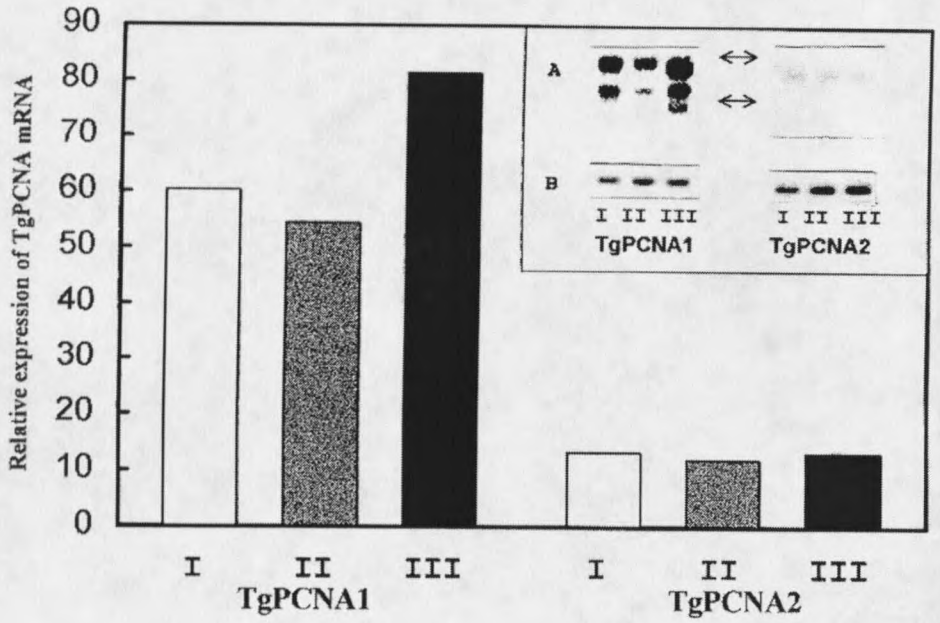

Figure 2-4. Relative levels of TgPCNA1 and 2 mRNAs from three different *T. gondii* tachyzoite strains. RH-Type I (I), ME49-PLK-Type II (II) and VEG-Type III (III) were quantified following normalization of RNA loading with a *T. gondii* 18S rRNA oligonucleotide probe. Inset A displays the autoradiographic results of hybridization with the TgPCNA probes. Two mRNA species are present for TgPCNA1 in Type I and II strains and three species are present in the Type III strain (inset blot A). TgPCNA2 (inset blot A) probe detected one mRNA species at a four to seven fold lower level of expression. The upper arrow indicates the location of the large subunit rRNA species (~28S) and the 18S rRNA is indicated by the lower arrow. Inset B displays the hybridization signal from reprobing each blot with a [^{32}P]-end labeled *T. gondii*-specific 18S rRNA oligonucleotide probe.

TgPCNA1 and 2 protein expression

Recombinant TgPCNA1 and 2 were purified to homogeneity from *E. coli* extracts on nickel columns and evaluated by SDS-PAGE. Due to the addition of N-terminal histidine tags, TgPCNA1 and TgPCNA2 migrated at 45 kDa and 42 kDa, respectively (Fig. 2-5, A). Purified proteins were used to generate anti-PCNA1- and 2-specific mouse polyclonal antibodies. Immune serum prepared from animals immunized

with recombinant TgPCNA1 reacted with TgPCNA1 but failed to recognize recombinant TgPCNA2 (Fig. 2-5, B- Lanes 1 and 2). Similarly, serum from TgPCNA2 immunized mice reacted only with TgPCNA2 recombinant protein (Fig. 2-5, B- Lanes 3 and 4). A two fold serial dilution of TgPCNA1 (Fig. 2-5, C) and TgPCNA2 (Fig. 2-5, D) recombinant protein demonstrated that each TgPCNA specific antisera has similar binding/affinity characteristics at the selected titer (1:2500). Preimmune mouse serum showed no reactivity against either recombinant protein (data not shown).

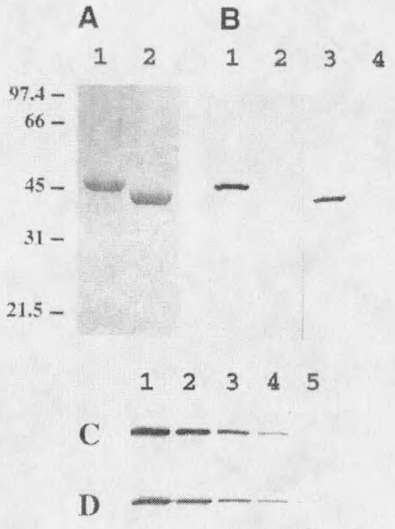

Figure 2-5. Cross reactivity of polyclonal antiserum to TgPCNA1 and 2 recombinant proteins. (A) Coomassie brilliant blue staining of affinity-purified (native conditions) recombinant TgPCNA1 and 2 (1.5 μg of each protein) separated on a 12% reducing SDS-PAGE gel. (B) Western blot analysis of polyclonal antisera produced against each TgPCNA recombinant protein. Lanes 1, 4 contain 30 ng of purified recombinant TgPCNA1; Lanes 2, 3 contain 30 ng of recombinant TgPCNA2. Lanes 1 and 2 were reacted with anti-TgPCNA1 (1:2,500) polyclonal serum and lanes 3 and 4 with anti-TgPCNA2 polyclonal serum (1:2,500). Molecular mass standards are indicated in kDa on the left. (C & D) Two fold serial dilution of TgPCNA1 (C) and TgPCNA2 (D) recombinant protein from 120 ng (lane 1) to 7.5 ng (lane 5) probed with the respective polyclonal antisera at identical titers (1:2500).

Anti-TgPCNA1 and 2 polyclonal antisera reacted with distinct antigens on Western blots of *T. gondii* tachyzoites from three genotypic strains. In contrast to the difference in mRNA levels, polyclonal antisera reactivity appeared similar in all extracts suggesting the levels of each TgPCNA protein are equivalent. Due to potential differences in antisera binding to native antigen, the absolute levels of TgPCNA proteins remain to be confirmed. In all three strains, anti-TgPCNA1 serum recognized an antigen of ~40 kDa (Fig. 2-6, lanes 1-3) corresponding to native TgPCNA1 without the 6xHis-tag. Likewise, anti-TgPCNA2 recognized a native PCNA2 that was 2-3 kDa smaller (~37 kDa) but expressed equally in the strains tested (Fig. 2-6, lanes 5-7). RH extracts were probed with a combination of anti-PCNA 1 and 2 sera (Fig. 2-6, lane 4) to verify the TgPCNA1 and 2 size differences. The slower migration of native TgPCNAs than what is predicted by cDNA coding size is likely due to anomalous electrophoresis that has been noted for other eukaryotic PCNAs [32]. The minor bands that are seen below the TgPCNA antigens (Fig. 2-6 non-specific) in all the lanes were detected in secondary antibody controls (data not shown).

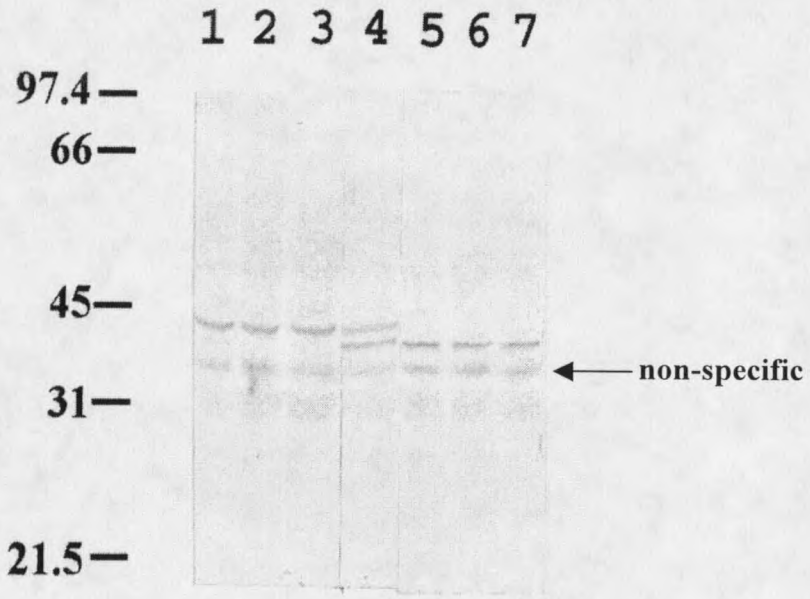

Figure 2-6. Western blot analysis of *T. gondii* tachyzoite lysates. Three genotypic lineages (RH, lanes 1, 4, 5; ME49-PLK, lanes 2, 6; VEG, lanes 3, 7) were electrophoresed under reducing conditions (12% SDS-PAGE) and incubated with TgPCNA specific antisera (1:2500). Lanes 1-3 were reacted with anti-TgPCNA1 serum and lanes 5-7 were reacted with anti-TgPCNA2. Lane 4 was incubated with an equal mixture of anti-TgPCNA1 and anti-TgPCNA2 antisera. Molecular mass standards are indicated in kDa.

Discussion

To facilitate studies of DNA replication in *Toxoplasma*, we have identified and characterized the expression of two PCNA genes in tachyzoites. Comparison of the putative TgPCNA1 and 2 coding sequences with PCNA from humans (Fig. 2-1) and other eukaryotes reveals the presence of conserved regions that include DNA binding motifs and replication-associated protein binding domains [8-9,28]. The C-termini of the TgPCNAs and PfPCNAs contain unique amino acids that extend the domain length

beyond that observed for human PCNA. This is significant because it has been suggested that the C-terminal region plays a key role in determining the specificity of PCNA interactions with other proteins associated with DNA replication, such as replication factor C and DNA polymerase δ [10].

Eukaryotic PCNAs are thought to form active clamp structures as homotrimers with a six-fold axis of symmetry as the result of having two globular domains per monomer [8]. Exceptions to this model may occur in the case of rare C-terminal extended domains as found in carrot and *Xenopus* [33-34] where these larger PCNAs may form a dimeric ring structure similar to the prokaryotic β-subunit clamp protein [12]. The presence of these alternate forms of PCNA is not well understood, however, they appear to be expressed in circumstances where cell division is unusually rapid [8]. The coding sequence of TgPCNA1 is predicted to encode a protein that contains a longer C-terminal domain than TgPCNA2 as well as human PCNA, and the relative size difference was confirmed by Western blot analysis (Fig. 2-6). Thus, TgPCNA1 may fit within the group of larger eukaryotic PCNAs, and therefore capable of forming different tertiary structures. The situation in Apicomplexa where two distinct forms of PCNA are simultaneously expressed in a single species provides a unique opportunity to explore the functional consequence of alternate PCNA structures.

Identification of two distinct PCNA genes within one species is unusual and to date has only rarely been observed in eukaryotes (with over 40 different species examined so far). In the eukaryotic family of PCNAs, two cDNAs have been identified only in carrots [33]. Examination of PCNA-like sequences in prokaryotic and viral genomes have revealed several duplications. *Paramecium bursaria* Chlorella virus 1

contains two putative PCNA-like sequences [35-36] and recent reports have identified two distinct β-subunit proteins (PCNA-like) in the Archea, *Sulfolobus solfataricus* [37].

Within *T. gondii*, the amino acid identity of TgPCNA1 and 2 is only ~27%, representing a higher degree of divergence than would be predicted by a recent duplication event. TgPCNA1 is in fact more similar to PfPCNA1 and CpPCNA1 (49 and 42% identity respectively) and likewise TgPCNA2 appears more related to PfPCNA2 and CpPCNA2. Thus, if these forms of PCNA arose from a single gene, the duplication likely occurred in the most common ancestor of *Toxoplasma*, *Plasmodium* and *Cryptosporidium* [38-39]. Mechanisms for duplicate gene acquisition are highly speculative, but one model involves horizontal gene transfer, and a recently published report suggests this process has been extensive among prokaryotes [40]. This is an intriguing hypothesis given the identification of two PCNA-like sequences in the genome of a virus that infects *P. bursaria* [35-36], a prokaryotic organism that may have similarities to the apicomplexan ancestor [38-39].

Given that the acquisition of two PCNAs in apicomplexan parasites is quite old, the question must be raised as to what has preserved their existence in the genome over time. Current models for the maintenance of a duplicated gene suggest a process whereby the duplicate gene mutates to acquire a new function (neofunctionalization) or both genes undergo rapid sequence divergence to a point where only partial function is retained (subfunctionalization) [41]. In the case of subfunctionalization, both genes are necessary to fulfill the function of the ancestral gene. Functional dissection of the TgPCNAs awaits further studies; however, preliminary cellular localization of ectopically expressed TgPCNA1 and 2 indicates each protein targets to the parasite nucleus (data not

shown) allowing for potential interaction. Analysis of TgPCNA1 and 2 mRNA levels demonstrate that in the tachyzoite stage both PCNA genes are actively transcribed (Fig. 2-4). Moreover, the expression pattern in all three *Toxoplasma* lineages demonstrate that PCNA expression is not genotypically restricted as has been found for the NTPase isoforms [29]. The difference in the number of mRNA species and comparative mRNA levels suggests each TgPCNA gene is independently controlled and alternative polyadenylation signals might be present in TgPCNA1. The experimental data presented here suggests that post-transcriptional control might be at work given the nearly equal levels of protein in spite of a 5-7 fold difference in mRNA levels.

References

1. Sibley LD, LeBlanc AJ, Pfefferkorn ER, Boothroyd JC. Generation of a restriction fragment length polymorphism linkage map for *Toxoplasma gondii*. Genetics 1992;132:1003-1015.

2. Sibley LD, Boothroyd JC. Construction of a molecular karyotype for *Toxoplasma gondii*. Mol Biochem Parasitol 1992a;51:291-300.

3. Sibley LD, Boothroyd JC. Virulent strains of *Toxoplasma gondii* comprise a single clonal lineage. Nature 1992b;359:82-85.

4. Ajioka JW, Boothroyd, JC, Brunk BP, Hehl, A et al. Gene discovery by EST sequencing in *Toxoplasma gondii* reveals sequences restricted to the Apicomplexa. Genome Res 1998;8:18-28.

5. Sheffield HG, Melton ML. The fine structure and reproduction of *Toxoplasma gondii*. J Parasitol 1968;54(2):209-226.

6. Dubey JP, Beattie CP. Toxoplasmosis of Animals and Man. Boca Raton, Florida: CRC Press 1988.

7. Makioka A, Ohtomo H. An increased DNA polymerase activity associated with virulence of *Toxoplasma gondii*. J Parasitol 1995;81(6):1021-1022.

8. Kelman Z. PCNA: structure, functions and interactions. Oncogene 1997;14:629-640.

9. Prosperi E. Multiple roles of the proliferating cell nuclear antigen: DNA replication, repair and cell cycle control. Prog Cell Cycle Res 1997;3:193-210.

10. Waseem HH, Labib K, Nurse P, Lane DP. Isolation and analysis of the fission yeast gene encoding polymerase δ accessory protein PCNA. EMBO J 1992;11(13):5111-5120.

11. Bauer GA, Burgers PMJ. Molecular cloning, structure and expression of the yeast proliferating cell nuclear antigen gene. Nucleic Acids Res 1990;18(2):261-265.

12. Kelman Z, O'Donnell M. Structural and functional similarities of prokaryotic and eukaryotic DNA polymerase sliding clamps. Nucleic Acids Res 1995;23(18):3613-3620.

13. Podust VN, Tiwari N, Stephan S, Fanning E. Replication Factor C disengages from proliferating cell nuclear antigen (PCNA) upon sliding clamp formation, and PCNA itself tethers DNA polymerase δ to DNA. J Biol Chem 1998;273(48):31992-31999.

14. Fukuda K, Morioka H, Imajou S, Ikeda S, Ohtsuka E, Tsurimoto T. Structure-function relationship of the eukaryotic DNA replication factor, proliferating cell nuclear antigen. J Biol Chem 1995;270(38):22527-22534.

15. Onrust R, Finkelstein J, Naktinis V et al. Assembly of a chromosomal replication machine: Two DNA polymerases, a clamp loader, and sliding clamps in one holoenzyme particle. J. Biol Chem 1995;270(22):13348-13357.

16. Morris GF, Mathews MB. Regulation of proliferating cell nuclear antigen during the cell cycle. J Biol Chem 1989;264(23):13856-13864.

17. Kilbey BJ, Fraser I, McAleese S, Goman M, Ridley RG. Molecular characterization and stage-specific expression of proliferation cell nuclear antigen (PCNA) from the malarial parasite, *Plasmodium falciparum.* Nucleic Acids Res. 1993;21:239-243.

18. Horrocks P, Jackson M, Cheesman S, White JH, Kilbey BJ. Stage specific expression of proliferation cell nuclear antigen and DNA polymerase δ from *Plasmodium falciparum.* Mol Biochem Parasitol 1996;79:177-182.

19. Roos DS, Donald RGK, Morrissette NS, Moulton ALC. Molecular tools for genetic dissection of the protozoan parasite *Toxoplasma gondii*. Meth Cell Biol 1995;45:25-61.

20. Howe DK, Sibley LD. *Toxoplasma gondii* comprises three clonal lineages: correlation of parasite genotype with human disease. J Infect Dis 1995;172:1561-1566.

21. Jerome ME, Radke JR, BohneW, Roos DS, White MW. *Toxoplasma gondii* bradyzoites form spontaneously during sporozoite-initiated development. Infect Immun 1998;66(10):4838-4844.

22. Wan KL, Blackwell JM, Ajioka JW. *Toxoplasma gondii* expressed sequence tags: insight into tachyzoite gene expression. Mol Biochem Parasitol 1996;75(2):179-186.

23. Thompson JD, Higgins DG, Gibson TJ. CLUSTAL W: Improving the sensitivity of progressive multiple sequence alignment through sequence weighting, position-specific gap penalties and weight matrix choice. Nucleic Acids Res 1994;22(22)4673-4680.

24. Felsenstein J. PHYLIP -- Phylogeny Inference Package (Version 3.2). Cladistics 1989;5:164-166.

25. Radke J, White MW. A cell cycle model for the tachyzoite of *Toxoplasma gondii* using the Herpes simplex virus thymidine kinase. Mol Biochem Parasitol 1998;95:237-247.

26. MacPherson JM, Gajadhar AA. Ribosomal RNA sequences for the specific detection of *Toxoplasma gondii* by hybridization assay. Molec Cell Probes 1993;7:97-103.

27. Harlow E, Lane D. Antibodies: A Laboratory Manual. Cold Spring Harbor: Cold Spring Harbor Laboratory Press, 1988.

28. Jónsson ZO, Hindges R, Hubscher U. Regulation of DNA replication and repair proteins through interaction with the front side of proliferating cell nuclear antigen. EMBO J 1998;17(8):2412-2425.

29. Asai T, Miura S, Sibley LD, Okabayashi H, Takeuchi T. Biochemical and molecular characterization of nucleoside triphosphate hydrolase isozymes from the parasitic protozoan *Toxoplasma gondii*. J Biol Chem 1995;270(19):11391-11397.

30. Gagnon S, Morency M-J, Bourbeau D, Levesque RC. *Toxoplasma gondii*: Structure and characterization of the 26S ribosomal RNA and peptidyl transferase domain. Exp Parasitol 1996;83:346-351.

31. Gagnon S, Levesque RC, Sogin ML, Gajadhar AA. Molecular cloning, complete sequence of the small ribosomal RNA coding region and phylogeny of *Toxoplasma gondii*. Mol Biochem Parasitol 1993;60:145-148.

32. Arroyo MP, Downey KN, So AG, Wang TSF. *Schizosaccharomyces pombe* proliferating cell nuclear antigen mutations affect DNA polymerase δ processivity. J Biol Chem 1996;271:15971-15980.

33. Hata S, Tsukamoto T, Osumi T, Hashimoto J, Suzuka I. Analysis of carrot genes for the proliferating cell nuclear antigen homologs with the aid of the polymerase chain reaction. Biochem Biophys Res Comm 1992;184(2):576-581.

34. Leibovici M, Gusse M, Bravo R, Mechali M. Characterization and developmental expression of Xenopus proliferating cell nuclear antigen (PCNA). Dev Biol 1990;141(1):183-192.

35. Lu Z, Li Y, Zhang Y, Kutish GF, Rock DL, Van Etten JL. Analysis of 45 kb of DNA located at the left end of the chlorella virus PBCV-1 genome. Virology 1995;206(1):339-352.

36. Li Y, Lu Z, Sun L, Ropp S, Kutish GF, Rock DL, Van Etten JL. Analysis of 74 kb of DNA located at the right end of the 330-kb chlorella virus PBCV-1 genome. Virology 1997;237(2):360-377.

37. De Felice M, Sensen CW, Charlebois RL, Rossi M, Pisani FM. Two DNA polymerase sliding clamps from the thermophilic Archeon *Sulfolobus solfataricus*. J Mol Biol 1999;291:47-57.

38. Cox FEG. The evolutionary expansion of the Sporozoa. Int J Parasitol 1994;24(8):1301-1316.

39. Roos DS, Crawford MJ, Donald RGK, Kissinger JC, Klimczak LJ, Streipen B. Origin, targeting, and function of the apicomplexan plastid. Curr Opin Micro 1999;2:426-432.

40. Jain R, Rivera MC, Lake JA. Horizontal gene transfer among genomes: The complexity hypothesis. Proc Natl Acad Sci USA 1999;96:3801-3806.

41. Force A, Lynch M, Pickett FB, Amores A, Yan Y, Postlethwait J. Preservation of duplicate genes by complementary, degenerative mutations. Genetics 1999;151:1531-1545.

CHAPTER 3

CHANGE IN THE PREMITOTIC PERIOD OF THE CELL CYCLE IS ASSOCIATED WITH BRADYZOITE DIFFERENTIATION IN *TOXOPLASMA GONDII.*

Introduction

In the United States, it is estimated that 1.5 million individuals are exposed annually to *Toxoplasma gondii* such that by age 50, there is a >35% chance of having contact with this pathogen [1]. While most of these infections are tolerated, *Toxoplasma* is dangerous to the unborn, to patients undergoing chemotherapy or organ transplant, and to people with AIDS [2-5]. As a result, toxoplasmosis is the third leading cause of foodborne deaths in the U.S. [1]. The unique ability of bradyzoites and tachyzoites to interconvert is considered to be the underlying cause of *Toxoplasma*-encephalitis in AIDS patients [4,6]. The bradyzoite form is slow growing, immunologically inert and not readily eliminated by the host immune system, and for this reason, in immune-compromised hosts, recurrent toxoplasmosis can occur each time latent bradyzoites recrudesce and proliferate as tachyzoites. Understanding the mechanism(s) that regulates development in this pathogen so that tachyzoite-to-bradyzoite interconversion may be prevented is of critical importance.

Several lines of evidence suggest that a developmental timer may operate in tachyzoite-to-bradyzoite switching, although the molecular details are not understood [7]. The differentiation of tachyzoites into bradyzoites occurs in conjunction with a change in

the cell cycle that happens spontaneously during emergence from a sporozoite infection [7] or is induced when tachyzoites are stressed [8-10]. Tachyzoites emergent from sporozoite-infections differentiate within a relatively tight window of proliferation, suggesting that the bradyzoite switch is linked to a division counting mechanism. Differentiation does not occur if tachyzoite growth is blocked [11], and thus, cell cycle progression is a prerequisite for development. However, it is unknown whether the switch to differentiate is restricted to a specific cell cycle phase.

Tachyzoite replication is characterized by a three-phase cell cycle comprised of G1 and S phases with mitosis following immediately upon the conclusion of DNA replication [11-12]. Parasite budding is evident with the formation of daughter apical/ inner membrane complexes which are well developed prior to nuclear division, and thus, budding may in fact initiate in S phase [11]. The S phase distribution of asynchronously growing tachyzoites is bimodal suggesting that chromosome replication may be nonuniform [11]. There is no evidence to support an extended G2 period in dividing tachyzoites, which is consistent with observations of other apicomplexans undergoing schizogony [13-17]. In this chapter, we demonstrate that bradyzoite recrudesence follows a developmental pathway, which is similar to development initiated by sporozoites. Furthermore, we describe a G2 population that arises during tachyzoite-to-bradyzoite differentiation, which is not detected in bradyzoite populations from mature tissue cysts.

Materials and Methods

Cell culture and parasite growth.

Human foreskin fibroblasts (HFF) were grown in Dulbecco's Modified Eagle Medium (Gibco BRL, Grand Island, NY) supplemented with 10% (v/v) fetal bovine serum (Atlanta Biologicals, Atlanta, GA). Sporulated oocysts from a Type III strain (VEG) were produced as previously described in Jerome et al. [7] and served as the source of inocula for sporozoite-initiated cultures. Parasites subjected to alkaline media (pH 8.3) were grown as described in Bohne et al. [18]. To produce tissue-cyst bradyzoites, CD-1 mice (Charles River Laboratories, Wilmington, MA) were inoculated (s.q.) with 3000 oocysts (VEG strain). Forty days post-inoculation the brains were removed from the cranial cavity and placed in phosphate buffered saline (PBS) at room temperature for two hours. Brain tissue was homogenized in 7.5 mls of PBS using a hand-held tissue grinder. Following homogenization, Percoll (Sigma, St. Louis, MO) was added to a final concentration of 24% (v/v) and the solution was centrifuged at 1875xg for 30 minutes. The cysts sedimented in the lower 1/3 of the gradient and were recovered by centrifugation at 1000xg for 10 minutes. The cysts were resuspended in 6 mls of PBS and filtered through a large pore screen followed by filtration through Nitex membrane. The cysts were washed from the top of the Nitex using 2-3 mls of PBS then pelleted at 1000xg for 10 minutes and resuspended in 0.5 ml of PBS. The bradyzoites were excysted for 20 seconds in excystation fluid (0.01 gm Pepsin, 0.2 gm NaCl and 0.0015% concentrated HCl). The excystation was stopped with the addition of DMEM

containing 10% FBS, and the bradyzoites were recovered by centrifugation at 1500xg for 15 min then resuspended in PBS.

Immunofluorescence analysis:

HFFs grown in 8-well chamber slides were inoculated with 10^5 parasites. At various intervals (2h, 18h, 24h, Day3 and Day 17) following parasite inoculation, parasites were washed in 1X phosphate buffered saline (PBS), fixed with 3.7% formyl saline and permeabilized with 0.25% Triton X-100. Rabbit polyclonal antiserum [19] specific for either TgPCNA1 (1:5,000) or TgPCNA2 (1:500) was added to the wells and incubated for 30 minutes. The wells were washed, fluorescein (FITC)-conjugated anti-rabbit immunoglobulin G diluted 1:100 (Sigma, St. Louis, Mo.) was added. The bradyzoite-specific monoclonal antibody BAG-1 (1:500) [20] recognizes a cytoplasmic antigen and was used to quantify the fraction of bradyzoites in each population. The mouse anti-BAG1 antibody was detected with phycoerethrin (PE)-conjugated anti-mouse IgG (Sigma, St. Louis, Mo.) diluted 1:64.

Surface antigen 1 (SAG-1) [21] expression in recrudescing parasites was analyzed by immunofluorescence analysis as previously described in Speer et al. [22]. Briefly, parasites were washed twice in 1X phosphate buffered saline (PBS), fixed with 3% paraformaldehyde for 30 min, treated in acetone for 10 min at 4°C, and air dried. The wells were treated with DG52 (α-SAG1, provided by Dr. J. Boothroyd) at 1:1,000 for 1 hour then washed with PBS and treated with fluorescein (FITC)-conjugated anti-rabbit immunoglobulin G diluted 1:100 (Jackson Immunoresearch, West Grove, PA). In all

experiments, the slides were evaluated with an epifluorescence microscope (Eclipse TE300, Nikon Inc., Melville NY), and images were collected with a digital camera (SPOT™, Dynamic Instruments Inc., Sterling Heights MI).

Fluorescent-Activated-Cell-Sorting (FACS).

Parasites were harvested for DNA content analysis by scraping monolayers, needle passing, filtering and pelleting (1300 x g). After harvest, parasites were fixed in ethanol and stored at –20°C for 24h prior to analysis [12]. Fixed parasites were resuspended in PBS and treated with 10 μg/ml propidium iodide (PI) (Sigma, St. Louis, MO) and 7.5μl of RNase cocktail (Ambion, Austin, TX) for 30 minutes in the dark. In order to examine the surface expression of SAG1 during bradyzoite development, ethanol fixed (>24 hr), parasites were centrifuged (1300 x g), re-suspended in 200 μl of anti-SAG1 antibody at 1:1000, and incubated on ice for 30 minutes. The parasites were washed (PBS), centrifuged as above, and treated with 200 μl of goat anti-mouse secondary IgG (FITC) at 1:250 (Jackson). Parasites were washed and resuspended in PBS for analysis. Two-color analysis of SAG1 expression versus DNA content was performed by staining the DNA following antibody treatment with 10 μg/ml PI and 7.5μl of RNase cocktail. Parasites were analyzed on a FACSCalibur flow cytometer (Becton-Dickinson Inc., San Jose CA). A minimum of 8,500 parasites was collected for analysis (collection rate of ~500-800cells/sec). Antibody fluorescence was collected on a log scale (FL-1 channel), while propidium iodide fluorescence was collected on a linear scale (FL-2).

Results

Expression of TgPCNA 1 and 2 during sporozoite-initiated development.

Parasite development in the intermediate host proceeds via the non-replicative sporozoite that differentiates into the rapidly growing tachyzoite ultimately giving rise to bradyzoites in the tissue cyst. At critical transitions, changes in growth rate signal the appearance of stage specific antigens, indicating that cell cycle mechanisms are somehow linked to the developmental program [7,20]. We have recently defined the major features of the tachyzoite cell cycle [11-12] in part through the use of immunfluorescent markers that are diagnostic of cell cycle phases. TgPCNA staining patterns are one set of markers used to detect parasites engaged in DNA synthesis—TgPCNA1 stipling and TgPCNA2 shuttling into the nucleus occurs in S phase parasites [11,19]. We have explored the changes in TgPCNAs during sporozoite-to-tachyzoite-to-bradyzoite development. TgPCNA1 was detected in the nucleus of all three developmental stages (Fig. 3-1 A-E) with the stipling characteristic of S phase occurring only in dividing tachyzoites (data not shown). Expression of TgPCNA2 was not evident in the newly excysted sporozoite (data not shown), but was detectable in parasites 18 h post-sporozoite inoculation (pre-replication) (Fig. 3-1 B). In emergent dividing tachyzoites, TgPCNA2 expression displayed the characteristic asynchronous pattern (~60% nuclear concentrated; 40% cytoplasmic) as reported (nuclear concentrated, Fig. 3-1 C) [19]. TgPCNA2 was detected in parasites at day 17 (Fig. 3-1 E) but similar to sporozoites (Fig. 3-1 B), parasites that co-expressed BAG1 at this stage of development no longer had TgPCNA2 concentrated

in the nucleus suggesting they were growth-arrested. This was corroborated by the low frequency of mitotic forms (double nuclei or internal daughters; [11,23]) in the $BAG1^+$ population (data not shown). In contrast, TgPCNA1 was concentrated in the nucleus regardless of the growth state.

Analysis of DNA content changes during sporozoite-initiated development.

Previously, we determined by FACS that VEG sporozoites possess a haploid genome, which is consistent with this cell cycle assignment; however, microfluorimetric measurements of *T. gondii* cystozoites were reported to have heterogenous genome contents indicating a more active cell cycle distribution [13]. We determined the DNA content by FACS of relatively pure populations of VEG strain sporozoites (from oocysts) (Fig. 3-2 A), emergent tachyzoites (day 3-post-sporozoite inoculation) (Fig. 3-2 B), and in bradyzoites from murine brain cysts (40 day post-oocyst inoculation) (Fig. 3-2 C). At least 10,000 events were collected for each population and the PI fluorescence of sporozoites was used as a standard for 1N DNA content upon which the other populations were compared. It is clear from these results that tissue cyst bradyzoites (Fig. 3-2 C) were more uniformly 1N than sporozoites, whereas, populations of emergent VEG tachyzoites displayed the characteristic fluorescence distribution of asynchronous replicating parasites [11-12].

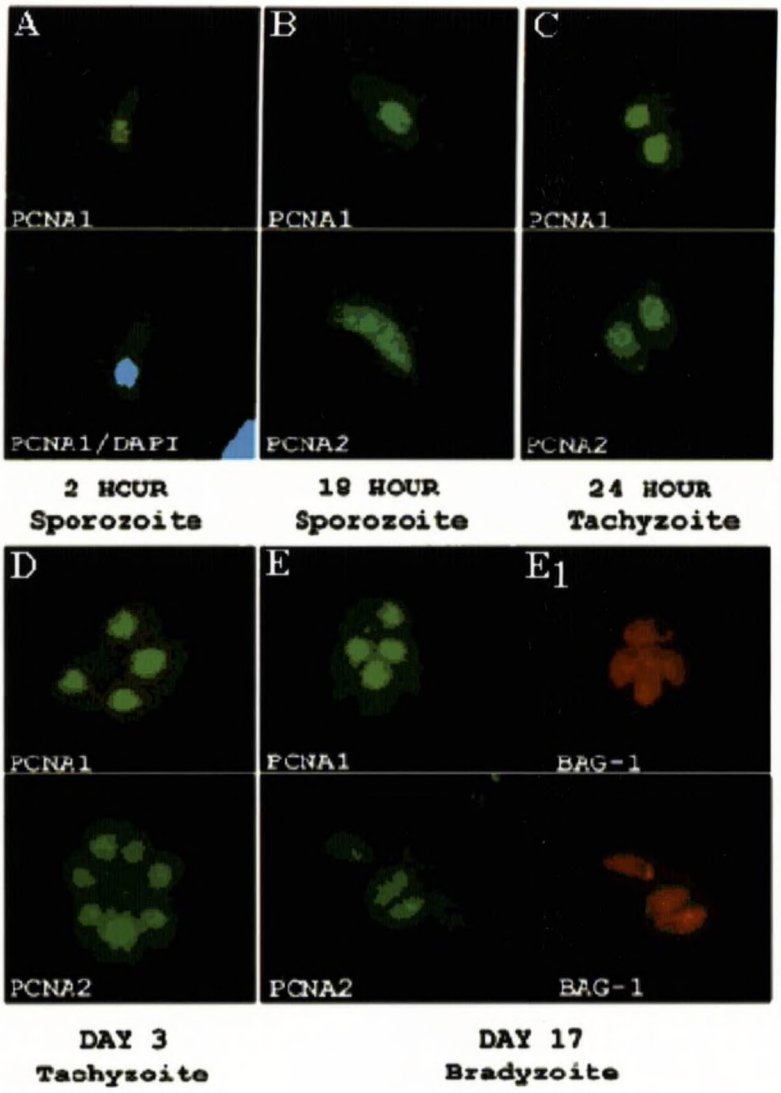

Figure 3-1. Developmental expression of TgPCNAs. (A) Sporozoites 2 h post-infection; (top panel) anti-TgPCNA1 antiserum, (bottom panel) overlay of anti-TgPCNA1 and DAPI counterstain. (B) Sporozoites 18 h post-infection; (top) anti-TgPCNA1, (bottom) anti-TgPCNA2. Homogenous, whole parasite staining of TgPCNA2 18 h post-infection is representative of the staining (2-24 h) prior to tachyzoite proliferation. (C) Newly emergent tachyzoites 24 h post-sporozoite infection, (top) anti-TgPCNA1, (bottom) anti-TgPCNA2. (D) Day 3 post-sporozoite infection, (top) anti-TgPCNA1, (bottom) anti-TgPCNA2. Nuclear recruitment of TgPCNA2 is evident in all proliferating populations Day-1-6 post-infection. (E) Day 17 parasites; (top panels) anti-TgPCNA1/anti-BAG1 (E_1), (bottom) anti-TgPCNA2/anti-BAG1 (E_1). Following the shift to slower growth there is no nuclear recruitment of TgPCNA2.

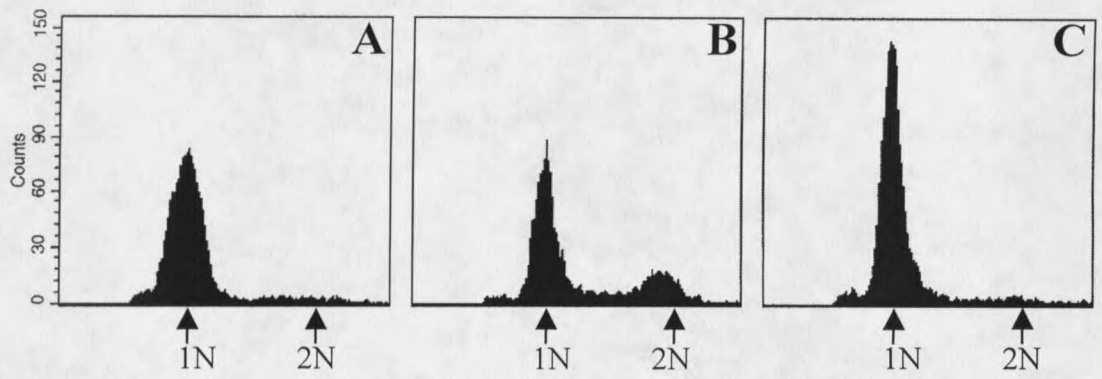

Figure 3-2. Flow cytometric analysis of sporozoite, tachyzoite and bradyzoite DNA content. Parasites were fixed in ethanol and stained with propidium iodide (10μg/ml) for 30 minutes. The histogram in each panel is the result of ~8500 events collected in the FL2-H channel. Arrows indicate 1N (peak mode FL2=400) and 2N (FL2=800) DNA contents. Sporozoites (A) and bradyzoites (C) are >95% 1N. Asynchronously growing tachyzoites (B) show the characteristic bimodal distribution [11].

In order to follow cell cycle changes of dividing tachyzoites as they differentiated into bradyzoites, we measured the DNA content by FACS and monitored a variety of cell cycle markers and the bradyzoite marker, BAG1, by immunofluorescence [11, 20] (Table 3-1). In this series of experiments, VEG tachyzoites emergent from sporozoite-infections were allowed to differentiate in HFFs spontaneously or were subjected to alkaline stress, which triggers a more synchronous and robust differentiation [7]. The cell cycle distributions of Day-3 tachyzoites (Table 3-1) served as a starting reference for these experiements [11]. Parasites at Day-9 post-sporozoite inoculation are growth-shifted [7], which was confirmed here by a higher fraction of parasites with 1N DNA complement (~71%) and a decrease in the proportion of S-phase parasites (Table 3-1). A shift in the fluorescence of the near-diploid subpopulation from an FL2-H mean of 735 (Day-3, parasite average value) to 759 was also noted. Evaluation of parallel cultures by

immunofluorescence assay (IFA), correlated well with the FACS results. Based on anti-TgPCNA1 staining, we determined that only 22% of the parasites contained the characteristic stipling pattern of S-phase [11], and the fraction of mitotic forms had also decreased (Table 3-1). At Day-9 post-sporozoite inoculation, we observed the first evidence that the proportion of 1.8-2N parasites was not correlated with the fraction of parasites in mitosis and cytokinesis. This was in contrast to synchronized RH^{TK+} parasites (RHΔ*hxgprt* parasites expressing an active thymidine kinase) [12] where changes in the fraction of 1.8-2N parasites occured in parallel with the proportion of parasites that were engaged in mitosis and cytokinesis [11-12]. As differentiation progressed in the VEG cultures, the fraction of 1.8-2N parasites increased such that by Day-15 post-sporozoite inoculation the population was comprised of 84% 1N and 15% 1.8-2N parasites with relatively small fractions containing characteristic S-phase (>1%), TgPCNA1 stippling or mitotic/cytokinetic forms (Table 3-1). The two predominate populations at Day-15 had average FL2-H values of 402 and 772, indicating they were much closer to the expected values for 1N and 2N contents, respectively. Similar results were obtained with sporozoite-infected cultures exposed to alkaline stress (96 h time-point shown here in Table 3-1). Nearly all of the parasites treated in pH 8.3 medium for 96 h expressed BAG1 (~99%), and the population could be divided into two major fractions based on DNA content; ~76% of the parasites were 1N (Table 3-1) and 21% were near-diploid (760 FL2-H) with relatively few parasites in S-phase or mitosis/cytokinesis.

Day	G1	S phase	G2	M/C	%BAG1$^+$
0	95	5	0	0	0
3	61	30	0	9	0
7	64	29	0	8	2
9	71	22	5	2	12
15	84	>1	15	>1	51
pH shift	76	3	21	>1	99

Table 3-1. Cell cycle and developmental distributions during sporozoite-to-bradyzoite differentiation. Parallel cultures were analyzed by flow cytometry (propidium iodide stain) and immunofluorescent microscopy to provide estimates of the proportion of parasites in G1, S, G2 and mitosis/cytokinesis (M/C) and to detect parasites that had begun to differentiate (BAG1$^+$). The proportion of S phase parasites was estimated by flow cytometric analysis and confirmed by counting nuclei that showed stipled anti-TgPCNA1 staining [11]. G2 parasites are defined here as the fraction of 1.8-2N parasites that are not accounted for by S-phase nuclei or parasites in mitosis/cytokinesis (double or u-shaped nuclei, daughter parasites). G1 was estimated from the proportion of 1N parasites. Sporozoite infected cultures were shifted pH 8.3 media at 72 hr post-inoculation and cell cycle distributions were determined 96 hr later.

Parasites expressing both SAG1 and BAG1 markers comprise most of the G2 fraction.

During tachyzoite-to-bradyzoite development a number of stage markers change expression in opposite directions; *e.g.* SAG1 decreases while BAG1 increases. Taking advantage of these markers, we employed a two color FACS analysis (Fig. 3-3) to evaluate 96 h alkaline-treated parasites for DNA content versus SAG1 expression. Identical cultures, prepared with the same sporozoite inoculum and alkaline medium were also analyzed for BAG1 expression. We found that virtually all the parasites in these cultures had begun to differentiate by 96 h (99% were BAG1$^+$ by IFA, data not shown). By FACS, 96 h alkaline-treated populations were heterogenous for the SAG1 marker, with 22.7% of the population at or below the background fluorescence cut-off (FL1 <15)

(Fig. 3-3 A, top). In contrast, undifferentiated tachyzoite populations were relatively homogenous for SAG1 expression as expected (Fig. 3-3 A, bottom). The DNA content of subpopulations, based on their SAG1 expression (Fig. 3-3 A, top) (bright, FL1>139 vs negative, FL1<15), demonstrated that the $SAG1^-$ parasites were primarily haploid (1N) (Fig. 3-3 B top) whereas, $SAG1^+$ parasites were comprised of nearly equal fractions of 1N (55%) and 2N (45%) (Fig. 3-3 B, bottom). Thus, the $SAG1^+$ subpopulation comprised most (85%) of the parasites that possesed a diploid genome in the differentiating population.

Bradyzoite de-differentiation is kinetically similar to development initiated by sporozoites.

Because mature sporozoites and bradyzoites appear to share an identical cell cycle pattern, we examined whether the bradyzoite-infection of HFF cells would follow a developmental course that was different or similar to that initiated by the sporozoite. Bradyzoites were purified from brain cysts of animals that had been infected with VEG oocysts 40 days prior to cyst harvest and inoculated into HFF monolayers. SAG1 and BAG1 expression and population growth-rate were followed in these cultures for a period of two weeks (Fig. 3-4). Bradyzoites purified from tissue cysts were $SAG1^-$ but re-expressed this marker by 18 h post-inoculation and prior to the onset of parasite replication in these cultures (Fig. 3-4 A). By 24 h, $SAG1^+$-parasites had begun to replicate and by 80 h a relatively fast growing tachyzoite population had emerged (Fig. 3-4). BAG1 expression steadily declined in these cultures and was undetectable by day 5.

Between Day 7 and 8 post-bradyzoite inoculation, the population spontaneously shifted to a slower growth rate (Fig. 3-4 B), and evidence of BAG1 expression was observed (Fig. 3-4 C). BAG1 expression increased in these populations such that by Day-15 the populations were again 75% positive for this antigen (Fig. 3-4 C).

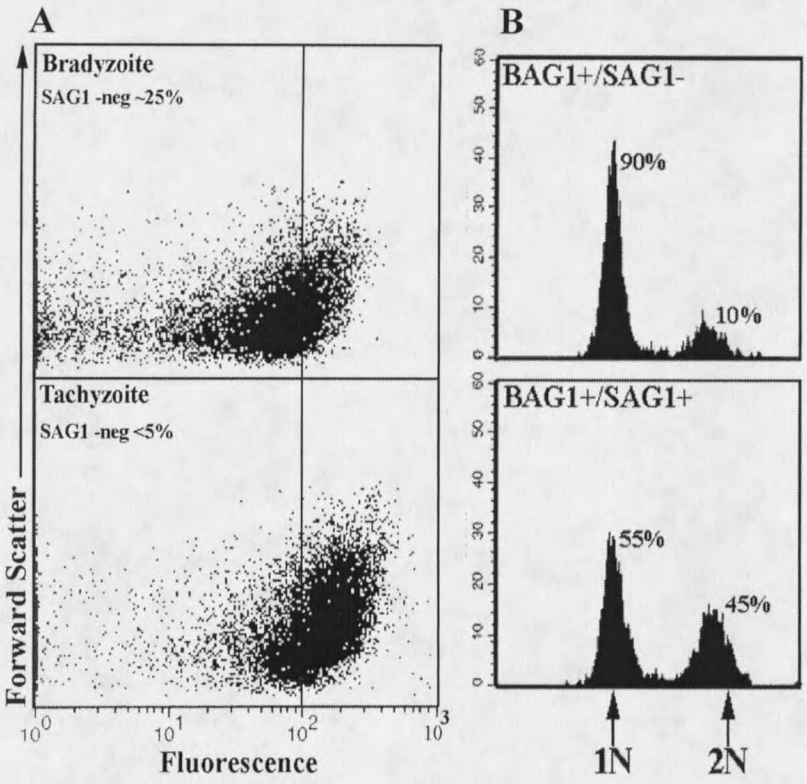

Figure 3-3. Two color flow cytometric analysis of differentiating parasite populations. Day-3 post-sporozoite VEG tachyzoites were shifted into pH 8.3 media for 96 hr and stained for the tachyzoite-specific marker SAG1 (mAB-DG52 [21]) (Panel A top) and DNA content with propidium iodide (panel B, top and bottom). Parallel cultures analyzed by immunofluorescence for the bradyzoite-specific marker BAG1 [20] showed that 99% of the parasites in these populations were BAG1+. Undifferentiated tachyzoites stained for SAG1 and analyzed by FACS are included here as a reference (panel A, bottom). Gated subpopulations in the differentiated cultures (panel A, top) were analyzed for DNA content (panel B). SAG1-negative parasites (FL1 <15) were 90% 1N (panel B, top), whereas SAG1-positive (FL1 >139) were divided nearly equally into 1N and 2N distributions (panel B, bottom). Note that the SAG1+, 2N parasites represent 85% on the total parasites that are diploid in this differentiated population. The DNA content of dull versus bright SAG1 parasites in the population of undifferentiated (A, bottom) tachyzoites were also analyzed and found to be identical (data not shown).

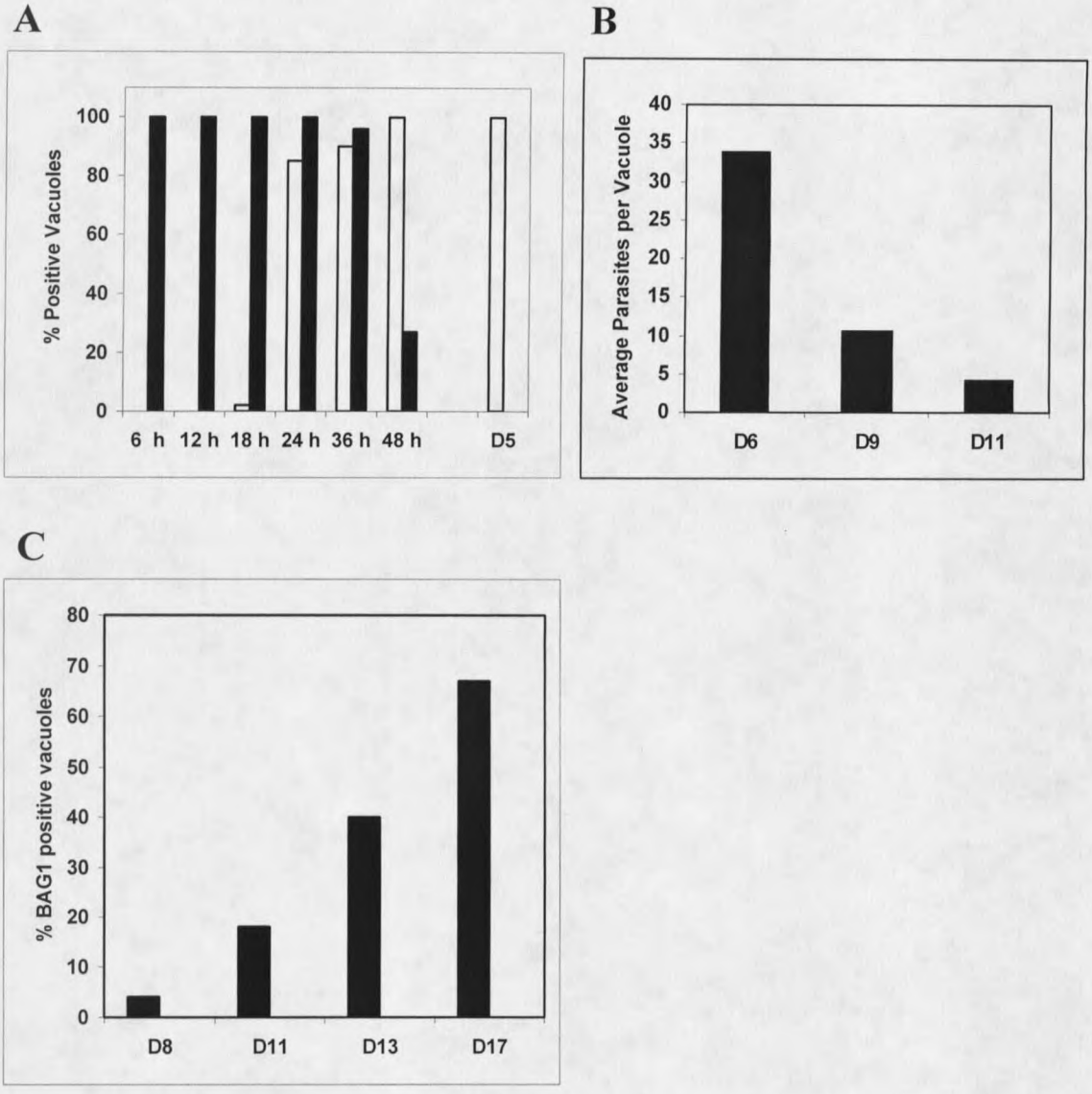

Figure 3-4. Analysis of the growth rate and BAG1 expression during recrudescence. (A) VEG strain bradyzoites purified from brain cysts were seeded into HFF monolayers and analyzed for BAG1 [20] (black bars) or SAG1 [21] (hatched bars) expression during the first 5 days post-inoculation. Note that SAG1 expression was first detected 18h post-inoculation and prior to the onset of parasite replication in these cultures. (B) Average vacuole size decreases as emergent tachyzoites shift to a slower growth phenotype day-6 post-bradyzoite infection. (C) The number of $BAG1^{+}$ parasites increases following the growth shift. D = Day, h = hours.

Discussion

The precise mechanisms that control apicomplexan development have not been uncovered, but like other protozoa, the results shown here are consistent with a link between chromosome replication and the parasite developmental pathway (Fig. 3-5 presents a cell cycle model for the *T. gondii* intermediate-host developmental pathway). VEG sporozoites (Day-0) are >90% haploid and do not begin to proliferate until ~20 hours post-inoculation, at which time their conversion into the tachyzoite is nearly complete [11-12]. At Day-3 (post-sporozoite), VEG tachyzoites replicate rapidly and display a DNA profile of ~60% 1N, ~30% 1N-2N, and ~10% 2N. The fraction of 2N parasites in Day 3-parasites corresponds closely to the number of parasites in mitosis and cytokinesis. A G2 population is undetectable at this time; however, as parasites reach growth restriction at Day-9, a new population (G2) emerges which contains a diploid DNA content and is not engaged in mitosis/cytokinesis. By Day-15 post-sporozoite infection, G2 parasites are ~15% of the population, while the other 85% contains a haploid DNA content. Alkaline shifted VEG parasites follow a similar, if abridged developmental course (Table 3-1). Here, 99% of the population express $BAG1^+$ four days post-sporozoite inoculation, indicating that the entire population has begun to differentiate, with some parasites intermediate ($BAG1^+/SAG1^+$) and others further along the pathway ($BAG1^+/SAG1^-$). Importantly, analysis of these parasites based on their SAG1 expression and DNA content (Fig. 3-3) demonstrates that the G2 population is predominately double positive ($BAG1^+/SAG1^+$). Parasites from tissue cysts are $SAG1^-$

and uniformly haploid, and thus, the G2 fraction in differentiating populations is likely an intermediate stage in the developmental pathway.

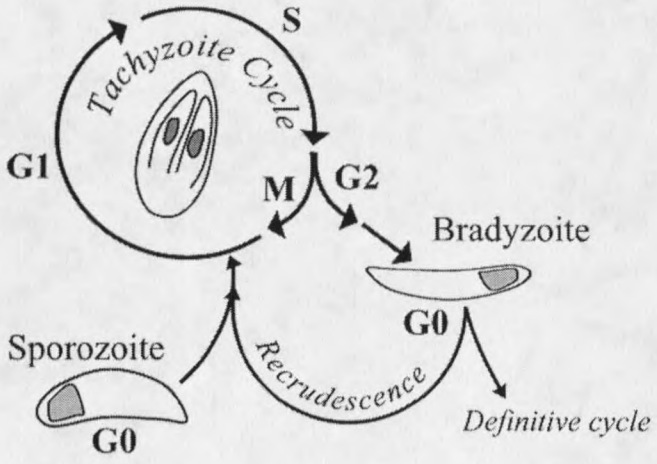

Figure 3-5. Model of *Toxoplasma gondii* development in the intermediate host.

The observation of VEG tachyzoite-to-bradyzoite develoment is consistent with a process whereby a change in the chromosome cycle is manifest by a late-S/G2 slowing or pause. Parasites emerging from this pause are committed to differentiate into bradyzoites. This process is likely stochastic, as suggested for differentiation of *Theileria* schizonts [24]. Thus, the probability of differentation is dependent on a change in the steady-state level of a factor(s) above (or below) a threshold margin. Consequently, differentiation is not synchronous as one or more cycles may be required to achieve the level needed to commit to differentiation. Laboratory-adapted strains, such as RH, have a fast cell cycle with a very short or non-existent G2, and therefore, a lowered potential to differentiate. Differentation does not occur if growth is blocked [11] because cell cycle

progression is required. Mechanisms that control protozoan chromosome replication are commonly intertwined with those that regulate cellular development. For example, it is well established that the differentiation of *Dictyostelium* and *Acanthamoeba* brought on by starvation conditions is triggered specifically when these protozoa occupy late-S phase/G2, suggesting DNA replication is likely a prerequisite for the change in developmental program [25-26]. Differentiation of *Trypanosoma brucei* in the bloodstream into procyclic forms [27], *Plasmodium* merozoite into gametocytes [28], *Theileria annulate* schizonts into merozoites [24], *Leishmania* amastigotes into promastigotes [29], and importantly, *T. gondii* tachyzoites into bradyzoites [8-10] are all induced to varying degrees by DNA synthesis inhibitors. In each of these models, changes in the chromosome cycle [30] (typically a slowing of DNA synthesis) appear crucial for development. It is thought that remodeling of nucleoprotein complexes may result when replication forks pass, and via this mechanism, changes in transcriptional patterns are connected to DNA replication [31]. Such a model has been proposed to account for the complex changes in the developmental program that occur during metazoan development [32] and could explain the link between DNA replication and protozoan development.

A prediction of the above model is that any condition that slows DNA synthesis appropriately has the potential to alter late-S/G2 and induce bradyzoite differentiation. This would explain why a variety of drugs with different modes of action induce differentiation in *T. gondii*. The model does not explain why sporozoite-derived tachyzoites spontaneously growth shift after ~20 divisions. Reconciliation of this question might be found when comparing early VEG tachyzoite division with higher

eukaryotic embryonic development. The events that follow fertilization are rapid nuclear division events controlled by a maternal cyclin [33-35]. The degradation of maternal cyclin regulates the timing and number of divisions in embryonic systems and dominates over the internal cycle of each cell. By analogy, factors carried in by the sporozoite or synthesized during sporozoite differentiation into the tachyzoite could similarly control the limited expansion of early tachyzoites revealing the underlying bradyzoite pathway only when their levels drop below a threshold. We have now demonstrated that de-differentation of bradyzoites back into tachyzoites (recrudescence) is kinetically indistinguishable from the sporozoite-induced developmental pathway (Fig. 3-4). Bradyzoites from *in vivo* tissue cysts differentiate into tachyzoites (as quantified by SAG1+ expression) in the same time-frame as sporozoites (12-18 h post-invasion) and only parasites that express tachyzoite markers proliferate. Like emergent tachyzoites from sporozoite-initiated infections, those emergent from bradyzoite inoculations grow relatively fast for a limited number of divisions and then they first spontaneously slow their growth and subsequently differentiate back into bradyzoites (Day-8 post-invasion). By Day-15 post-bradyzoite inoculation, 75% of the population has re-expressed the bradyzoite-specific antigen BAG1. Thus, a single cell cycle mechanism may control both branches of the intermediate life cycle of *T. gondii*.

Collectively, these data and data presented in Jerome et al. [7] and Radke et al. [11] represent investigations into the relationship between the cell and developmental cycle of the *Toxoplasma* intermediate life stage. The model put forth (Fig. 3-5) describes the complete developmental life cycle with respect to the cell cycle. Sporozoites are in a G0 state and differentiate into the tachyzoite which proliferates by means of a three stage cell

cycle [11], then tachyzoites differentiate into bradyzoites by entering a G2 period prior to the final mitotic event that leads to the growth-arrested bradyzoite (Fig. 3-5). Bradyzoites can de-differentiate, re-enter the cell cycle and apparently follow the same developmental pathway used by the sporozoite.

References

1. Mead PS, Slutsker L, Dietez V, McCaig IF et al. Food-related illness and death in the United States. Emerg Infect Dis 1999;5:607-625.

2. Chan ISF, Neaton JD, Saravolatz LD, Crane LR, Osterberger J. Frequencies of opportunistic diseases prior to death among HIV-infected persons. AIDS 1995;9:1145-1151.

3. Martinez AJ, Sell M, Mitrovics T, et al. The neuropathology and epidemiology of AIDS, a Berlin experience. A review of 200 cases. Path Res Pract 1995;191:427-443.

4. Tenter AM, Heckeroth AR, Weiss LM. *Toxoplasma gondii*: from animals to humans. Int J Parasitol 2001;30:1217-1258.

5. Jones JL, Kruszon-Moran D, Wilson M, Mcquillan G, et al., *Toxoplasma gondii* Infection in the United States: Seroprevelance and Risk Factors. Am J Epidem 2001;154(4):357-365.

6. Luft BJ, Remington JS. Toxoplasmic encephalitis in AIDS. Clin Infect Dis 1992;15:211-222.

7. Jerome ME, Radke JR, BohneW, Roos DS, White MW. *Toxoplasma Gondii* Bradyzoites Form Spontaneously during Sporozoite-Initiated Development. Infect Immun 1998;66(10):4838-4844.

8. Soete M, Camus D, Dubremetz JF. Experimental induction of bradyzoite-specific antigen expression and cyst formation by the RH strain of *Toxoplasma gondii in vitro*. Exp Parasitol 1994;78:361-370.

9. Bohne W, Hessemann J, Gross U. Reduced replication of *Toxoplasma gondii* is necessary for induction of bradyzoite-specific antigens: a possible role for nitric oxide in triggering stage conversion. Infect Immun 1994;62:1761-1767.

10. Soete M, Fortier B, Camus D, Dubremetz JF. *Toxoplasma gondii*:kinetics of bradyzoite-tachyzoite interconversion in vitro. Exp Parasitol 1993;76(3):259-264.

11. Radke JR, Striepen BS, Guerini MN, Jerome ME, et al. Defining the cell cycle of the tachyzoite stage of *Toxoplasma gondii*. Mol Biochem Parasitol 2001;115:165-175.

12. Radke J, White MW. A cell cycle model for the tachyzoite of *Toxoplasma gondii* using the Herpes simplex virus thymidine kinase. Mol Biochem Parasitol 1998;95:237-247.

13. Cornelissen AWCA, Overdulve JP, Van Der Ploeg M. Determination of nuclear DNA of five Eucoccidian parasites, *Isospora* (*Toxoplasma*) *gondii, Sarcocystis cruzi, Eimeria tenella, E. acervulina and Plasmodium berghei*, with special reference to gamonto-genesis and meiosis in *I.* (*T.*) *gondii*. Parasitol 1984;88: 531-553.

14. Fujishima M. Microspectrophotometric and autoradiographic study of the timing and duration of pre-mitotic DNA synthesis in *Paramecium caudatum*. J Cell Sci 1983;60:51-65.

15. Canning EU, Morgan K. DNA synthesis, reduction, and elimination during life cycles of the Eimeriine Coccidian, *Eimeria tenella*, and the Haemogregarine, *Hepatozoon domerquei*. Exp Parasitol 1975;38:217-227.

16. Jacobberger JW, Horan PK, Hare JD. Cell cycle analysis of asexual stages of erythrocytic malaria parasites. Cell Prolif 1992;25:431-445.

17. Irvin AD, Ocama JGR, Spooner PR. Cycle of bovine lymphoblastoid cells parasitosed by Theileria parva. Res Vet Sci 1982;33:298-304.

18. Bohne W, Hunter CA, White MW, Fergusson DJ, et al. Targeted disruption of the bradyzoite-specific gene BAG-1 does not prevent tissue cyst formation in *Toxoplasma gondii*. Mol Biochem Parasitol 1998;92(2):291-301.

19. Guerini MN, Jerome M, Kvaal C, White MW. Proliferating-cell-nuclear-antigens of *Toxoplasma gondii* are dissimilar in expression and potential function. Manuscript in preparation.

20. Bohne W, Gross U, Ferguson DJ, Heesemann J. Cloning and characterization of a bradyzoite-specifically expressed gene (hsp30/bag1) of *Toxoplasma gondii*, related to genes encoding small heat-shock proteins of plants. Mol Microbiol 1995;16(6): 1221-1230.

21. Kim KK, Bulow R, Kampmeier J, Boothroyd JC. Conformationally appropriate expression of the *Toxoplasma antigen* SAG1 (p30) in CHO cells. Infect Immun 1994;62(1):203-209.

22. Speer CA, Tilley M, Temple ME, Blixt JA, Dubey JP, White MW. Sporozoites of *Toxoplasma gondii* lack dense-granule protein GRA3 and form a unique parasitophorous vacuole. Mol Biochem Parasitol 1995;75(1):75-86.

23. Morrissette, NS, Bedian, V., Webster, P. and Roos, DS. Characterization of extreme apical antigens from *Toxoplasma gondii*. Experimental Parasitology 1994;79:445-459.

24. Shiels B, Aslam N, McKellar S, Smyth A, Kinnaird J. Modulation of protein synthesis relative to DNA synthesis alters the timing of differentiation in the protozoan parasite *Theileria annulata*. J Cell Sci 1997;110:1441-1451.

25. Jantzen H, Schulze I. Relationship between the timing of DNA replication and the developmental competence in *Acanthamoeba castellanii*. J Cell Sci 1988;91-389-399.

26. Weeks G, Weijer CJ. The *Dictyostelium* cell cycle and its relationship to differentiation. FEMS Micro Lett 1994;124:123-130.

27. Mutomba MC, Wang CC. Effects of aphidicolin and hydroxyurea on the cell cycle and differentiation of *Trypanosoma brucei* bloodstream forms. Mol Biochem Parasitol 1996;80:89-102.

28. Ono T, Ohnishi Y, Nagamune K, Kano M. Gametocytogenesis induction by Berenil in cultured *Plasmodium falciparum*. 1993;77:74-78.

29. Sacks DL, Perkins PV. Identification of an infective stage of *Leishmania* promastigotes. Science 1984;223:1417-1419.

30. Nasmyth K. Control of S phase. In:Concepts in Eukaryotic DNA replication. (DePamphilis, M.L. ed) Cold Spring Harbor Laboratory Press 1999:331-386.

31. Wolffe AP. Chromatin structure and DNA replication:Implications for transcriptional activity. In:Concepts in Eukaryotic DNA replication. (DePamphilis, M.L. ed) Cold Spring Harbor Laboratory Press 1999:271-293.

32. Edgar LG, McGhee JD. DNA synthesis and the control of embryonic gene expression in *C. elegans*. Cell 1988;53:589-599.

33. Ducommun B. From growth to cell cycle control. Semin Cell Biol 1991;24(4):233-41.

34. Hunt T. Cyclins and their partners:from a simple idea to complicated reality. Semin Cell Biol 1991;2(4):213-222.

35. Pines J. Cyclins:wheels within wheels. Cell Growth Differ 1991;2(6):305-310.

CHAPTER 4

PROLIFERATING-CELL-NUCLEAR-ANTIGENS OF *TOXOPLASMA GONDII* ARE DISSIMILAR IN EXPRESSION AND POTENTIAL FUNCTION.

Introduction

DNA replication in eukaryotic and prokaryotic cells requires a scaffold onto which the replisome assembles and is stabilized [1-3]. In prokaryotes, the β-subunit serves this role whereas eukaryotes utilize proliferating-cell-nuclear-antigen (PCNA) [4]. Although PCNA was initially mis-assigned as a cyclin, its core function is to increase the processivity of DNA polymerase, and in some cells, the cycling of PCNA is coincident with the turnover of cyclin complexes [5]. Within the eukaryotic replisome, PCNA functions as a sliding clamp through which chromosomal DNA passes and upon which delta polymerase can process lengthy templates [6-7]. Given its central position in DNA metabolism, it is not surprising that PCNA has been demonstrated to play a role in DNA repair, cell cycle control, transcriptional regulation, and chromatin assembly [6-7]. Consequently, attempts to delete the PCNA gene have been unsuccessful because it is essential to cell division [8-9].

Our laboratory previously described two unique PCNAs [Chapter 2 and ref. 10] in the protozoans, *Toxoplasma gondii* and *Plasmodium falciparum*. The PCNAs from *T. gondii* are distinct, and more similar to each of their counterparts in *P. falciparum* than they are to each other, suggesting they did not arise from a simple gene duplication [10].

Expression of TgPCNA1 and 2 was detected in tachyzoite strains representing the three genotypic lineages, and each PCNA appears to be encoded by a single gene. The occurrence of multiple PCNAs has been found in the genome analysis of *Cryptosporidium parvum* [M. Abrahamsen, personal communication, Chapter 2], a related apicomplexan, and *Drosophila melanogaster* [11]. Genomic sequencing of thermophilic Archea have uncovered several instances of multiple genes encoding diverse β-subunits [12-13]. No significance for having multiple PCNAs, such as a gain or division of function, has emerged from studies of cells that possess two copies of PCNA. Multiple β-subunits from two bacteria [12-13] have been cloned; however, only subtle differences in their respective activities have been noted [12-13].

In the studies presented here, we demonstrate that *Toxoplasma* TgPCNA1 and 2 are differentially expressed with respect to the tachyzoite cell cycle and that each PCNA forms homotypic but not heterotypic interactions, indicating they likely act independently. We also provide evidence that TgPCNA1 likely serves as the major replisomal PCNA in this microorganism as it is capable of complementing the PCNA function in yeast and appears to be essential in *Toxoplasma*.

Materials and Methods

Cell culture and parasite growth

Human foreskin fibroblasts (HFF) were grown in Dulbecco's Modified Eagle Medium (Gibco BRL, Grand Island NY) supplemented with 10% (v/v) fetal bovine serum (Atlanta Biologicals, Atlanta GA). The *T. gondii* strain RHΔ*hxgprt* [14] was used as the parental strain for gene knockout experiments.

Production of Antibody Reagents

TgPCNA1 and 2 coding regions were cloned into pQE-30 (Qiagen, Chatsworth CA) expression vectors in order to produce recombinant proteins as described [10]. Immune serum for each TgPCNA was prepared by immunizing New Zealand White rabbits with 100 μg of purified recombinant TgPCNA (rTgPCNA) in Hunter's Titermax® adjuvant (Sigma, St. Louis MO). The antisera was titered and verified for TgPCNA specificity as described in Guerini et al. (2000).

Cell cycle specific expression of TgPCNA 1 and 2

TgPCNA protein localization was examined in synchronized RH^{TK+} tachyzoites (RHΔ*hxgprt* parasites expressing an active thymidine kinase) [15]. HFF's were infected with ~80,000 RH^{TK+} tachyzoites in 8-well chamber slides. Following 16 hours of

growth, exogenous thymidine [10 μM] was added to the media and monolayers were incubated an additional 4h at 37°C allowing the RH^{TK+} parasites to arrest at the G1/S boundary. Replacing the thymidine containing media with normal 1% DMEM releases the parasites from the block thereby allowing the synchronized population to proceed through at least one complete cell cycle. The intracellular localization of PCNA1 and 2 was determined by immunofluorescence imaging. Parasites were washed in 1X phosphate buffered saline (PBS), fixed with 3.7% formyl saline and permeabilized with 0.25% Triton X-100. Wells in each slide were treated with either α-TgPCNA1 (1:10,000) or α-TgPCNA2 (1:500) rabbit polyclonal antisera for 30 minutes, washed and then treated with fluorescein (FITC)-conjugated anti-rabbit immunoglobulin G diluted 1:100 (Sigma, St. Louis, Mo.). Parasites were simultaneously stained with anti-mouse C4F3 antibody at 1:500 [16] and 4,6-diamidino-2-phenylindole (DAPI, 0.16 μg/μl) to detect daughter apical complex formation and nuclear division. The mouse anti-C4F3 antibody was detected with secondary antibody phycoerethrin (PE)-conjugated anti-mouse IgG (Sigma, St. Louis, Mo.) diluted 1:64. The slides were evaluated with an epifluorescence microscope (Eclipse TE300, Nikon Inc., Melville NY), and images were collected with a digital camera (SPOT™, Dynamic Instruments Inc., Sterling Heights MI).

TgPCNA1 and 2 protein interaction

Recombinant TgPCNA1 and 2 were allowed to interact at physiological temperature (37°C) and pH (7.5). Prior to electrophoresis the recombinant proteins were incubated 15 min. in 0.5 M Tris (pH 7.5) at 37°C [17] and loaded in native sample buffer (62.5 mM Tris, pH 6.8, 40% glycerol, 0.01% Bromophenol Blue). Homotypic and heterotypic interactions were detected by Coomassie Blue staining following electrophoresis on a 4-15% gradient gel (Bio-Rad, CA) under native conditions at 10°C [17].

TgPCNA1 and 2 interaction was also assessed by yeast two-hybrid analysis. TgPCNA coding regions were amplified from cDNA [10] using the polymerase chain reaction (PCR) and cloned (TgPCNA1, *EcoRI/SalI*; TgPCNA2, *EcoRI/XhoI*) into pBD-GAL4 Cam phagemid vector (Stratagene, La Jolla CA). The pBD-GAL4 has the tryptophan (W) selectable marker. TgPCNA1 and 2 were both cloned into the pAD-GAL4-2.1 phagemid vector (Stratagene) using *EcoRI/XhoI*. This vector can be selected for in yeast by using the Leucine selectable marker. The four plasmid combinations (two homotypic and two heterotypic) were transformed into yeast strain YRG-2 using LiAc [18] and plated on media lacking leucine and tryptophan (SC -W-L). Protein interaction was assessed on yeast complete medium lacking histidine (SC –W-L-H).

Transcomplementation of a cold-sensitive *S. cerevisiae* POL30 (PCNA) mutant

The *Saccharomyces cerevisiae* strain PY 44-52, contains a cold sensitive mutation in the POL30 gene (yeast PCNA) (kindly provided by Dr. Burgers, [19]). In order to test the ability of TgPCNA1 or 2 to complement this defect in yeast, TgPCNA coding regions were cloned into a plasmid (pMET426) [20] that contains a selectable marker (URA) and an inducible promoter (MET). Strain PY44-52 was transformed individually with each TgPCNA and, following selection on media lacking uracil (–Ura), single colonies were inoculated onto two selective medias (-Ura –Met or -Ura + 1.3 μM methionine) and incubated at 15°C.

Generation of TgPCNA gene "knockout" constructs

T. gondii genomic clones for TgPCNA 1 and 2 were isolated from a λDASH-II genomic library (AIDS Research and Reference Reagent program, Cat. No 2863) and the flanking, exon and intron structures were sequenced. To prepare the TgPCNA1 knockout construct [21-22], a 6.5 kb genomic fragment was cloned into pBluescript KS+ and the hypoxanthine-xanthine-guanine phosphoribosyl transferase (HXPGRT) [14] minigene was subcloned into a unique *Mun*I site in exon 4. Similarly, a 10.2 kb genomic fragment spanning the TgPCNA2 locus was cloned into pBluescript KS+ and an ~3.3 kb region (*BamHI*/*Mun*I) encompassing exons 4 and 5 was replaced with the HXGPRT minigene. The linearized targeting constructs (50 μg) were transfected into 10^7 parasites by

electroporation, as previously described [23], and stable transformants were selected using 50 μg ml^{-1} mycophenolic acid and 50 μg ml^{-1} xanthine. After two rounds of selection, parasites were cloned in 96-well plates by limiting dilution in the presence of drug selection. TgPCNA1 knockouts were screened by PCR of genomic DNA using primers 5'-GGCTGGAGATGAGTCGCAGG-3' (TgPCNA1-gP1Fya; sense) and 5'-CCCTCTG-CGTCATCCACACC-3' (TgPCNA1-TgPCNA1 revKO; antisense), while TgPCNA2 knockouts were identified with primers 5'-CCGAGCAACTGGAAGTCCC-3' TgPCNA2-P2; sense) and 5'-GGGGGCAAGACAGCGAGTCAC-3' (TgPCNA2-P2r21c; antisense).

Analysis of TgPCNA2 "knockout" parasites

To confirm TgPCNA genetic deletions, genomic DNAs were isolated and Southern analysis was DNA performed. Additionally, total RNA was prepared from RHΔ*hxgprt* and TgPCNA2 knockout parasites by TRIzol (Gibco-BRL, Grand Island NY) extraction and analyzed by Northern blot for the presence of TgPCNA2 mRNA. Hybridization was performed at 42°C for 16h in a solution containing 50% formamide and 6 X SSC using [^{32}P]-labeled inserts. Following hybridization, nitrocellulose blots were washed three times in 2 X SSC containing 0.1% SDS at room temperature (10 min each) and then twice in 0.1 X SSC containing 0.1% SDS at 42°C (30 min each). Blots were exposed to x-ray film at -80°C. Southern blots were hybridized with either the 6.5 kb TgPCNA1 or 10.2 kb TgPCNA2 genomic fragments labeled with [^{32}P] by nick-

translation. The probes used for Northern analysis represent a single divergent region of each TgPCNA that is capable of distinguishing each mRNA species [10].

A variety of methods were used to characterize TgPCNA2 knockout parasites. Growth rate and virulence were tested as described in Jerome et al. [24]. The DNA content of parasites was measured using flow cytometry [25]. After harvest, parasites were fixed in ethanol and stored at –20°C for 24h prior to analysis then resuspended in PBS and treated with 10 μg/ml propidium iodide (PI) (Sigma, St. Louis, MO) and 7.5μl of RNase cocktail (Ambion, Austin, TX) for 30 minutes in the dark. A variety of cell cycle markers were used to visualize parasite growth, including markers for daughtrer parasite formation (C4F3) [16] and nuclear division [25]. The ability of parasites to differentiate into bradyzoites was examined under alkaline conditions (pH 8.3) [26].

Two biochemical strategies were employed to assess *in vitro* DNA synthesis [17] and incision repair [27]. DNA polymerase activity from protein extracts of "knockout" and "wt" parasites was analyzed by measuring product length resulting from the extension of an oligo dT primer (18 bases) annealed to a polydA template (size range 300 to 100 nucleotides) annealed at a ratio of 20:1 (poly dA:primer/ μg:μg) [17]. The reaction was incuabated at 37°C for 90 minutes in the presence of gamma ^{32}P-labeled TTP and then stopped by the addition of SDS, extracted with phenol:chloroform and denatured for 10 minutes in buffer containing 90% formamide. Products were electrophoresed on a 6% denaturing (8M Urea) polyacrylamide gel in 1X TBE then the gel was exposed to x-ray film at -80°C. Products were analyzed for both length and radiolabel incorporation. The incision repair assay used the same protein extracts and the

template consisted of two oligos (one containing a mis-match) annealed together and a radiolabeled nucleotide. Products were electrophoresed on a 15% polyacrylamide gel and exposed to x-ray film at -80°C for analysis.

The frequency of non-homologous integration was measured in "knockout" and parental parasites using the plasmid p*min*CAT [28] which contains the chloramphenicol selectable marker. Following electroporation, selection was carried out in chloramphenicol (20 μM) and parasites were plaqued to determine viability and integration. Stable integration was reported as the number of chloramphenicol resistant parasites/number of viable parasites.

Results

TgPCNA2 is transported in and out of the nucleus during parasite replication

As mammalian and yeast cells progress through a single division cycle, PCNA was shown to localize to the nucleus concurrent with replication foci building and firing [29]. To study the localization of TgPCNA1 and 2 during the cell cycle [15, 25], we analyzed synchronized RH^{TK+} tachyzoites [15] using rabbit antisera specific for TgPCNA1 or 2. At all cell cycle stages TgPCNA1 fluorescence remained concentrated in the nucleus (Fig. 4-1 -◇-), and as demonstrated previously, TgPCNA1 displayed a stippling pattern in those parasites that were in S-phase [25]. The localization of TgPCNA2 changed with respect to the cell cycle phase (Fig. 4-1). In asynchronous tachyzoite populations, TgPCNA2 was concentrated in the nucleus of ~61% of the

parasites and this number increased (>80%) in parasites blocked in late G1/early S phase (Fig. 4-1, -■- nuclear, late G1/earlyS, inset A). The remaining 20% of the parasites from the blocked population showed no evidence of nuclear localization (Fig. 4-1, -▲- cytoplasmic, inset B). As synchronized parasites transited S phase and entered mitosis, the fraction of parasites with TgPCNA2 concentrated in the nucleus steadily decreased to less than 20% of the population. Thus, TgPCNA2 is distinct from TgPCNA1 in that it concentrates in the nucleus only during late G1 and S phases and in other stages of the cell cycle it is distributed throughout the parasite cytoplasm.

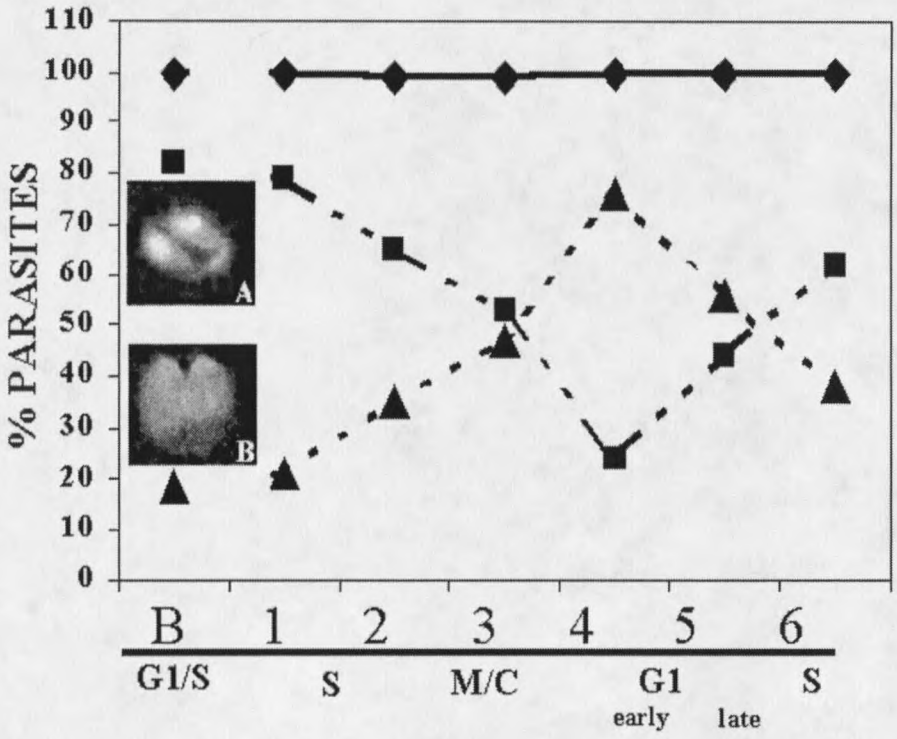

Figure 4-1. The cellular distribution of TgPCNA changes during the tachyzoite cell cycle. RH^{TK+} tachyzoite growth was synchronized with thymidine (4h block) at the G1-S boundary of the cell cycle (B). At hourly intervals from 1-6 h post thymidine release (points 1-6), parasites were stained with TgPCNA 1 or 2 specific antisera in order to determine the cellular location of each protein in 100 vacuoles picked at random. Inset A and B show representative changes in the TgPCNA2 staining patterns during the course of tachyzoite division.

TgPCNA1 and 2 form homotypic but not heterotypic complexes

PCNA in human and yeast cells is thought to function as a homotypic trimer that encircles DNA during replication [6-7, 17, 30]. The expression of distinct PCNAs in *Toxoplasma* raises the question of whether TgPCNA1 or TgPCNA2 also interact, either separately or with one another, to form a multimeric structure. To explore this question, we determined whether purified recombinant proteins might interact under native conditions *in vitro* [17] or in a yeast two-hybrid assay. Recombinant TgPCNAs were incubated separately or in equal mixtures and then resolved on native gels. By itself, rTgPCNA1 remains primarily monomeric (Fig. 4-2A, lane 2) with approximately 5-10% of the total protein migrating at a molecular mass consistent with dimerization (Fig. 4-2A, band a). Conversely, rTgPCNA2 alone readily forms a homodimer (Fig. 4-2A, band b) with a small amount of monomer and trimer (Fig. 4-2A, band c) also evident in these gels. When rTgPCNA1 and rTgPCNA2 were combined (Fig. 4-2A lane 4) the protein complexes were additive of the patterns seen individually (compare Fig. 4-2A lane 4 with lanes 2, 6). No new complexes were detected nor were there any apparent shifts in the complexes, suggesting rTgPCNA1 and 2 do not interact.

To independently confirm this pattern of interaction, we analyzed TgPCNA1 and 2 binding in the yeast two-hybrid system. For analysis of homotypic interactions, plasmids (binding domain (BD) and activation domain (AD)) containing either TgPCNA1 (1-BD:1-AD) or TgPCNA2 (2-BD:2-AD) were co-transformed into yeast strain YRG-2. Additionally, TgPCNA1 and 2 in BD and AD plasmids were co-transformed into yeast giving the following two heterotypic combinations (1-BD:2-AD

and 2-BD:1-AD). The interaction between TgPCNA1 fused with the activation and bait domains reconstituted the GAL4 transcription factor and activated expression of the *HIS*3 reporter gene allowing yeast to grow on synthetic complete media lacking histidine (Fig. 4-2B, right plate). Likewise, TgPCNA2 fused to both domains grew on selective media (Fig. 4-2B, right plate). Thus, both sets of homotypic interactions found in the recombinant protein system are confirmed with the two-hybrid approach. In contrast, yeast co-transformed with the heterotypic plasmid combinations did not grow in either configuration (Fig. 4-2B, right plate).

TgPCNA1 but not TgPCNA2 complements a POL30 yeast mutant

Unsuccessful attempts to generate *POL30* (PCNA) deletion mutants in yeast demonstrate that PCNA is an essential gene [9]. *S. cerevisiae* strain PY44-52 [19] is a PCNA (*POL30*) cold sensitive mutant that is capable of growth at 30°C but not at 15°C (Fig. 4-3, left panel, top and bottom). To determine whether TgPCNA1 or 2 could complement PY44-52, their coding regions were cloned downstream of the methionine repressible promoter in vector pMET426 [20]. PY44-52 cells transformed with pMET426-TgPCNA1 were able to grow at 15°C in low methionine demonstrating that TgPCNA1 is capable of rescuing the *POL30* mutation in yeast (Fig. 4-3, right panel, bottom). As little as 1.3 μM methionine blocked TgPCNA1 complementation at the restrictive temperature (data not shown). In contrast, PY44-52 was not rescued by pMET426-TgPCNA2 (Fig. 4-3, right panel, bottom), although these transformants grew normally at 30°C in methionine-deficient medium indicating heterologous TgPCNA2 expression in yeast is not toxic.

A

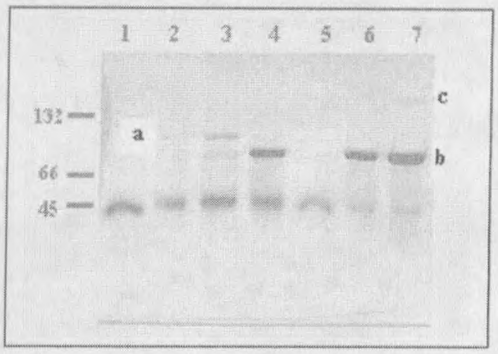

B

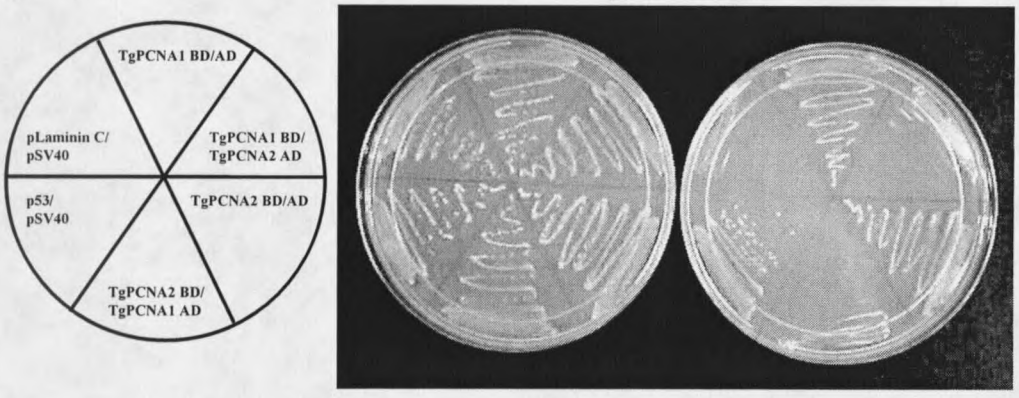

Figure 4-2. TgPCNA1 and 2 form homotypic but not heterotypic complexes. (A) Recombinant TgPCNA1 and 2 or a mixture of both proteins were separated on a 4-15% native gradient gel at 15°C; 5 μg (lane 2) or 10 μg (lane 3) of TgPCNA1 alone, 5 μg (lane 6) or 10 μg (lane 7) TgPCNA2 alone, or a mixture (5 μg each) of both proteins (lane 4). Each protein (5 μg) was run under reducing conditions in order to provide a reference for monomeric TgPCNA1 (lane 1) and TgPCNA2 (lane 5). (B) Yeast two-hybrid analysis of TgPCNA protein interactions. Bait (TgPCNA1-BD, TgPCNA2-BD) and prey (TgPCNA1-AD, TgPCNA2-AD) plasmids were constructed, co-transformed into yeast strain YRG-2, and selected on selective (SC –L -W) media (middle panel). Colonies were streaked onto SC-L-W-H (right panel) to assay for fusion protein interaction. Homotypic TgPCNA1 or 2 co-transformants grew on triple selection media whereas in either heterotypic configuration (1-AD/2-BD or 2-AD/1-BD) no growth was detected. Positive (pSV40-AD/p53-BD) and negative (pSV40-AD/Laminin C-BD) controls displayed the correct phenotype.

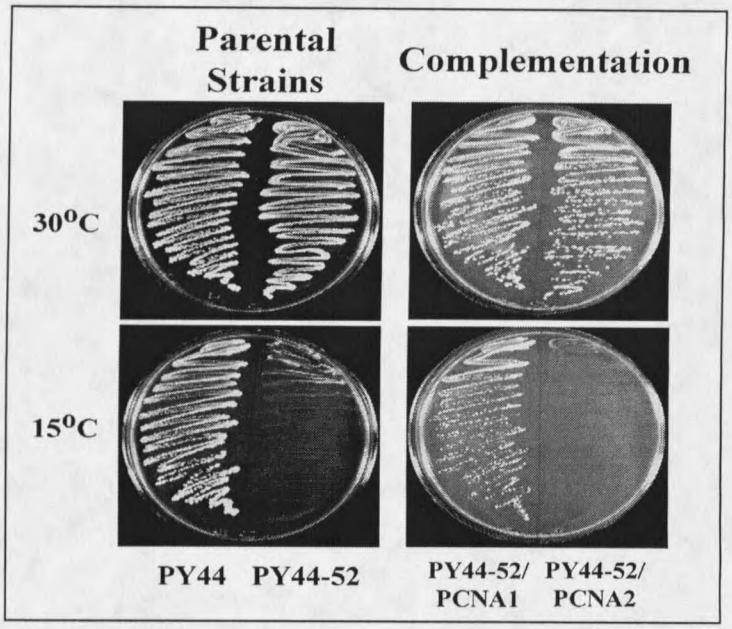

Figure 4-3. TgPCNA1 complements a *POL*30 (PCNA) mutant yeast strain. *S. cerevisiae* strain PY44-52 contains a mutation in the *POL*30 (PCNA) gene such that growth occurs at 30°C but not at 15°C. The parental strain PY44 is capable of growth at both temperatures. Plasmids containing the protein coding sequence of TgPCNA1 or 2 were placed under the control of the yeast promoter MET25 were transformed into PY44-52 (right panels). TgPCNA1 complemented the defect in PY44-52 (growth at 15°C, right panel) while TgPCNA2 did not.

Generation of TgPCNA gene "knockouts"

Although PCNA is thought to be essential to cell growth in eukaryotes, this has only been demonstrated in cells that contain a single PCNA species [8-9]. To examine this question in *T. gondii*, we have attempted to produce a single gene deletion of each TgPCNA. The *Toxoplasma* PCNA1 gene is comprised of four similar sized exons and three introns (Fig. 4-4A). The TgPCNA2 gene has a different composition, which is consistent with the concept that these genes were acquired independently. The

TgPCNA2 locus consists of five exons and four introns. The fourth exon is very small (82 nucleotides) while the fourth intron spans 1280 nucleotides (Fig. 4-4B), which appears to be more than twice the average intron size in this parasite.

RHΔ*hxgprt* parasites were electroporated with a ▲TgPCNA2 construct (Fig. 4-4B), selected in media containing 50μg ml^{-1} mycophenolic acid and 50μg ml^{-1} xanthine and then cloned by limiting dilution in 96 well plates. From a total of 192 clones examined by PCR for a gene replacement, clones #3, 53 and 90 were identified as putative TgPCNA2 knockouts (~1:66). Southern analysis of the three TgPCNA2 knockout clones confirmed they contained a single gene replacement (Fig. 4-5A). Further characterization of clone #3 by Northern analysis verified the absence of TgPCNA2 mRNA (Fig. 4-5B) in this mutant.

An attempt to delete the TgPCNA1 gene was also undertaken using both "hit-and-run" mutagenesis [21-22], and homologous gene replacement as was done for TgPCNA2. Neither strategy resulted in a TgPCNA1 gene replacement. The "hit-and-run" mutagenesis provided 29 clones, and seven were confirmed as pseudodiploids. However, several attempts to generate a gene replacement by negative selection (6-thioxanthine at 320 μg/ml) were unsuccessful. Direct gene replacement was also attempted, and while TgPCNA2 knockouts were found at a frequency of 1 in 66 mycophenolic acid resistant clones, no TgPCNA1 replacements were found in >200 clones examined.

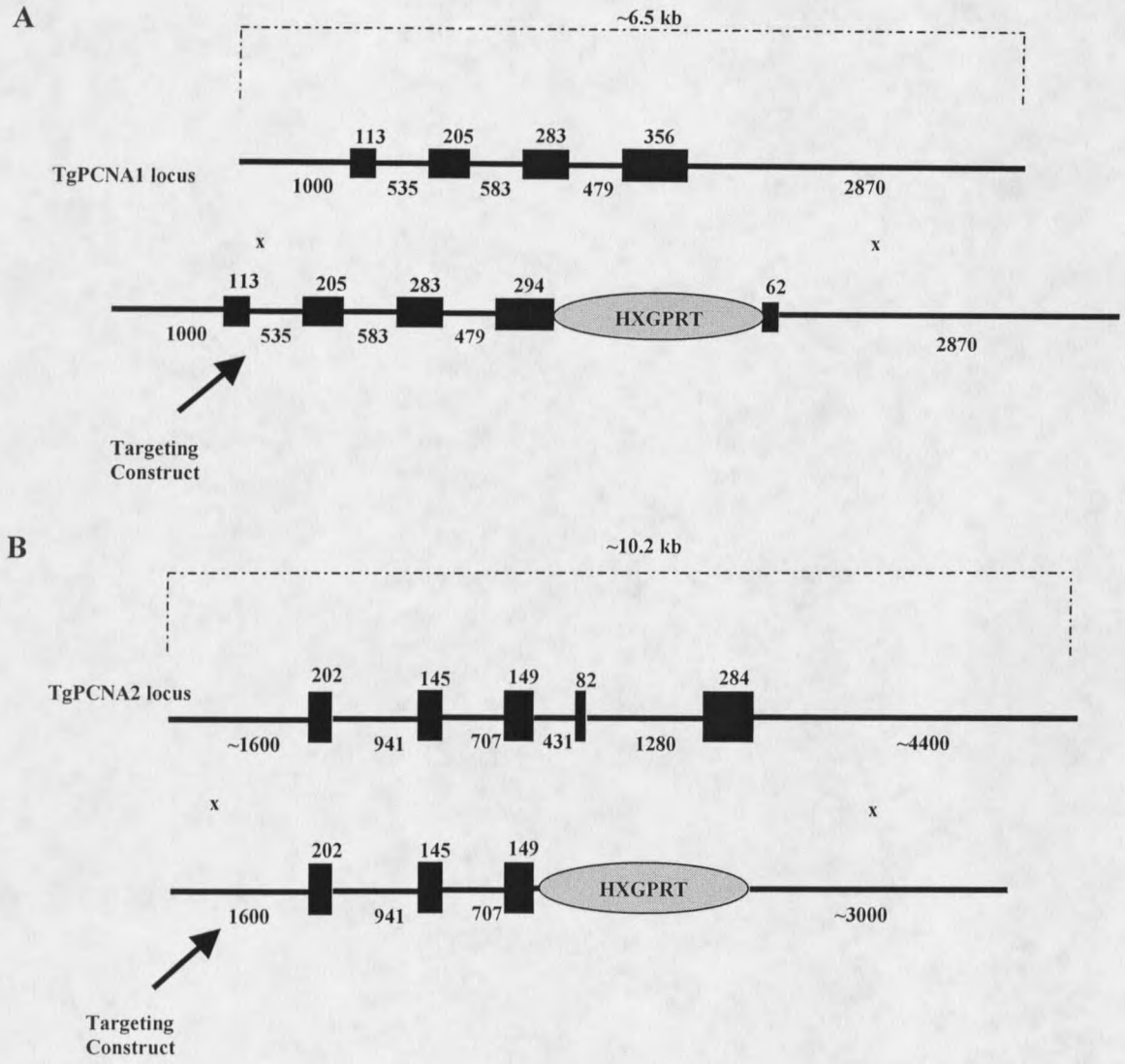

Figure 4-4. Genetic structures of TgPCNA1 and 2 and targeting construct designs. (A) The gene for TgPCNA1 is comprised of four exons and three introns. (B) TgPCNA2 gene has five exons and four introns.